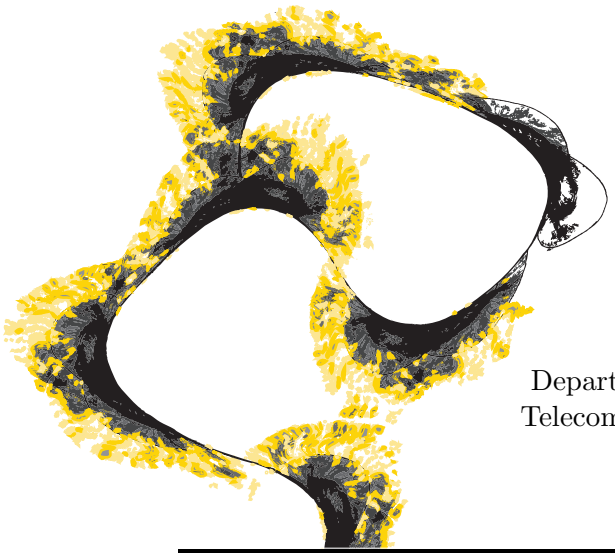

University of Twente
Department of Electrical Engineering
Telecommunication Engineering Group

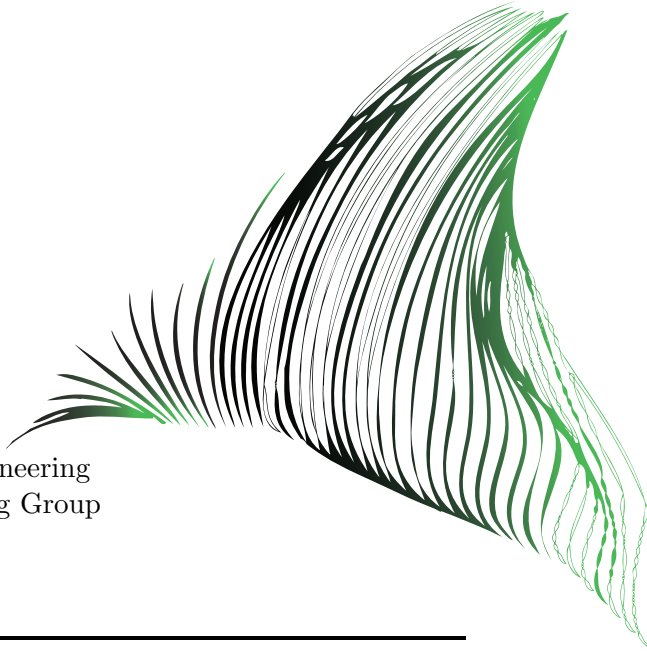

Design of an Astronomy Front End for Orbiting Low Frequency Antennas for Radio Astronomy

by
Robert Grootjans

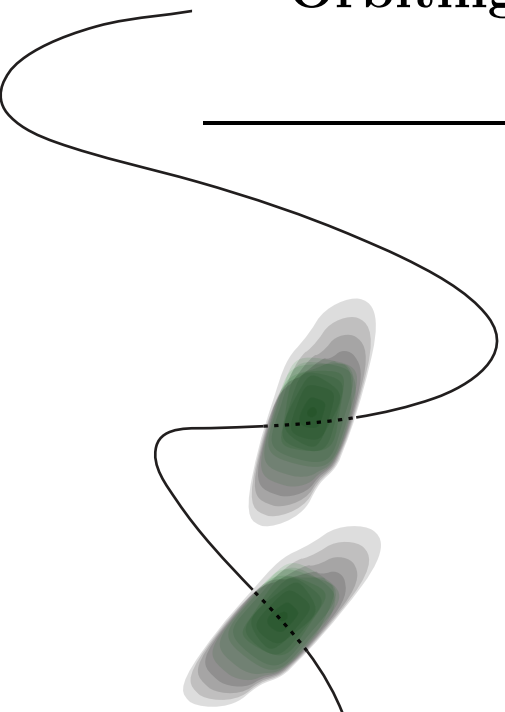

Master Thesis
June 2016

Supervisors:
Dr. ir. M.J. Bentum
Prof. dr. ir. ing. F.B.J.C. Leferink
Dr. ir. G.H.C. van Werkhoven
Dr. ir. R.A.R. van der Zee
Dr. ir. A. Budianu

June 22, 2016

Abstract

The Orbiting Low Frequency Antennas for Radio Astronomy satellite cluster initiative was started to explore a new area of low-frequency radio astronomy. Due to the partial or complete opaqueness of the atmosphere for frequencies below 30 MHz, this initiative plans to form a swarm of antenna nodes in space. These nodes will also experience less radio frequency interference than they would on Earth. This thesis explores the steps needed to make a viable front end within the tight boundaries of a 3U cubesat. Existing antennas are modeled and examined. This is followed by system calculations to specify the astronomical front-end for an OLFAR node concretely. Once the specifications are known, a wideband amplifier topology is presented and simulated. Finally, the design is proven to be suitable for OLFAR and is ready for realisation. A viable front end is presented and simulated, and it can be concluded that this front end mostly meets the specifications.

List of abbreviations

ADK Antenna Design Kit

ADS Advanced Design System

ARU Astronomical Receiver Unit

ARU Astronomical Receiver Unit

CMRR Common Mode Rejection Ratio

CMRR Common Mode Rejection Ratio

COTS Commercial Off The Shelve Components

DSP Digital Signal Processor

ENOB Effective Number Of Bits

EOR Epoch of Re-ionisation

GBW Gain-Bandwidth

HFSS High Frequency Structural Simulator

HPBW Half Power Beam Width

IP3 Third order intercept point

IXR Intrinsic Cross Polarisation Ratio

LNA Low Noise Amplifier

OLFAR Orbiting Low Frequency Antennas for Radio astronomy

opamp operational amplifier

PSRR Power Supply Rejection Ratio

RFI Radio Frequency Interference

SAS Smart Antenna System

SAW Surface Acoustic Wave

SFDR Spurious Free Dynamic Range

TRAC Triangular Retractable and Collapsible

Contents

Chapter 1

Introduction

These days, radio astronomy science is an important factor in the scientific process of discovering aspects of the universe. A lot of radio astronomy instruments already exist, ranging from large dishes to phased array antenna systems. An example of this is the low frequency array (LOFAR) project spearheaded by ASTRON [1]. The newest initiative is the construction of the low frequency array called the Square Kilometre Array Low Frequencies (SKA-low) [2]. The reason scientists are interested in low-frequency radio astronomy is that this is an uncharted portion of the sky. Scientists hope to find out about the time closest to the big bang, called the Epoch of Re-ionisation [3]. They also hope to fins out more about the Dark Ages of the Universe, the time between the Big Bang and the EOR. Also studies about exoplanets and the interstelllar medium are in the scope of OLFAR [4].

(a) LOFAR (The Netherlands)

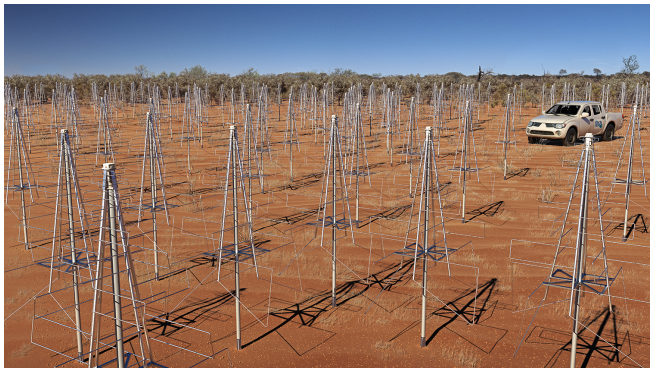

(b) SKA (Western Australia)

However, low-frequency radio astronomy has a few drawbacks. First of all the wavelength of the signals is in the order of tens of meters, meaning that usually large antennas are needed (or synthetic apertures in the case of array antennas). Usually this is done by creating large arrays instead of single dish antennas. Secondly for very low frequencies, the Earth's ionosphere blocks frequencies below 30 MHz [5]. An impression of the observable spectrum available to observe on Earth can be seen in Figure 1.2.
To overcome this problem, initiatives based on satellite systems have been proposed. Because of the large baselines needed for low frequencies, array antennas are the only feasible option in space. The DARIS project researched the feasibility of satellite swarms in space [7]. The Orbiting Low Frequency Antennas for Radio Astronomy (OLFAR) project is an initiative by University of Twente, Technical University of Delft, ASTRON and some other small companies [8]. OLFAR plans to place a swarm of satellites into a moon orbit [8]. The purpose of these satellites is to function as a distributed low frequency array far away from man made radio frequency interference (RFI) and away from the blocking ionosphere. An impression of a satellite swarm can be seen in Figure 1.3.

Constructing an array in space brings new challenges. It is quite costly to send equipment into space. A crude indicator is that it costs about 20000 USD per kg to send into space [10]. Due to this cost, it is important to keep the satellites as small as possible. The cubesat platform is chosen because the individual satellites are small, simple and replaceable [8]. However, it does mean that you are dealing with a limited power budget and size constraints.

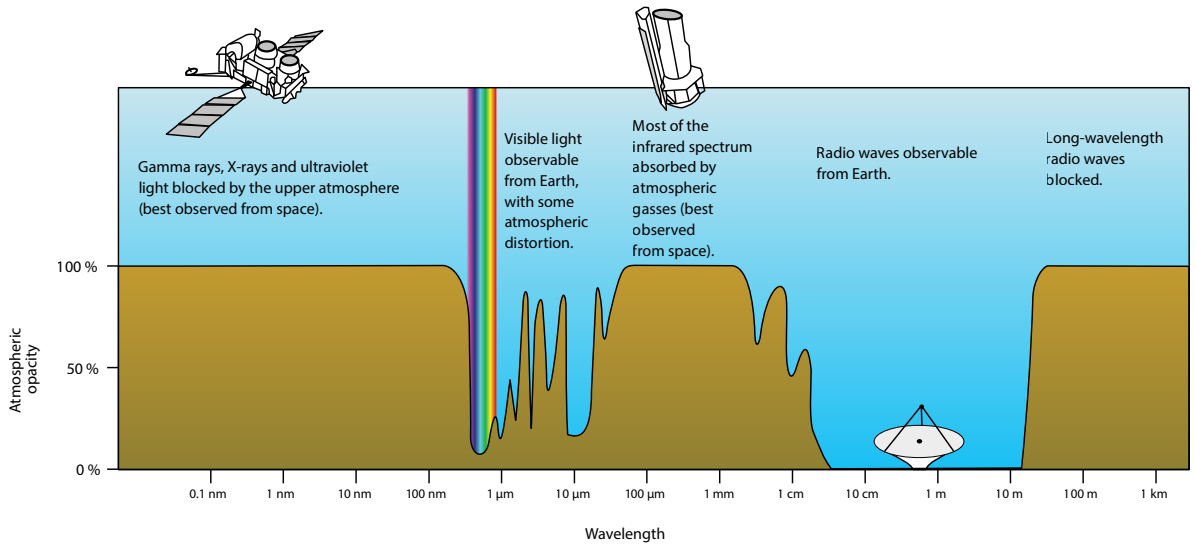

Figure 1.2: Atmospheric opacity for different wavelengths [6].

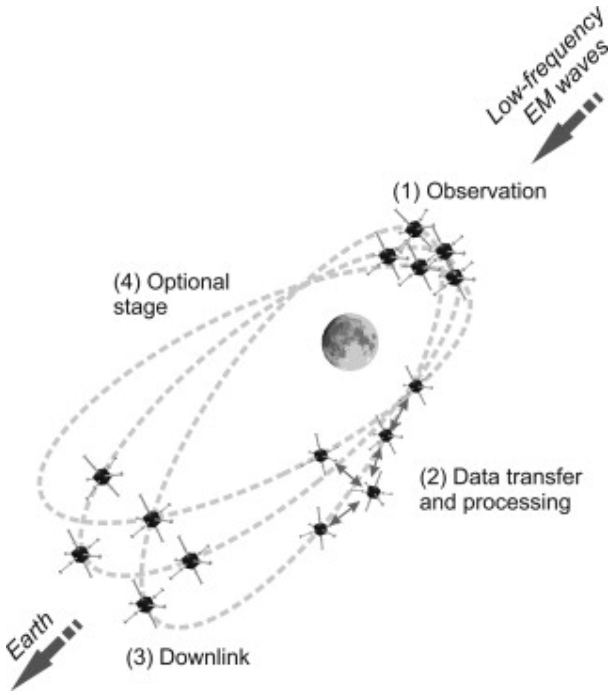

Figure 1.3: The OLFAR swarm concept, the swarm orbits around the moon and has four different stages. 1) In the observation stage the swarm functions as an astronomy instrument. 2) In the Data transfer and processing stage the signal is correlated and prepared for downlink. 3) In the downlink stage the data is sent to earth. 4) The optional stage is available for other potential tasks. [9].

In this Master Thesis, the focus will lie on the astronomical front end of a single OLFAR satellite (from now on referred to as 'node'). An OLFAR node or station is defined as a 3U cubesat that functions as an autonomous unit in the distributed array. The usage of self-sustaining autonomous nodes is important because it inherently increases redundancy in a system of many nodes. In the case of OLFAR, the initial size is 10 nodes, and eventually will expand to a size of 50 nodes. Another advantage of using small satellites is that it is easy to mass-produce, also the size and cost of the nodes can be kept to a minimum. [5]

The designed front-end will function as the interface between space and the digital domain. As stated, the observed signals are from unknown astronomical sources. These signals will be picked up by an antenna (for example the antenna designed by K.A. Quillien in [11]) and analysed by [12]. After that, the signals are amplified and filtered by the receiver. Finally, the signals will be converted to a digital signal using an analogue to digital converter (ADC), and are further digitally processed by the satellite. The power source of the satellite are solar panels deployed from the side of the satellite. The amount of power this power source gives is stated in the OLFAR straw man design [13]. As stated before the format of the satellite is a 3U cubesat format. 1 U means a cubic frame with sides 10 cm long. The eventual goal is to combine the antenna system with the receiver, and digital processing to one complete science instrument.

1.1 Research Question

The goal of this project is to design an astronomical front-end for OLFAR nodes. This will involve primarily the design, dimensioning and possible realisation of the antennas and also the design of an antenna Low Noise Amplifier (LNA). For this master research project, the research question is:

How does one implement an astronomical front end for OLFAR keeping in mind the tight constraints on the cubesat platform?

This research question can be divided in to a set of sub questions:

- What is the optimal antenna length and diameter?
- What is the optimal antenna configuration?
- How should the receiver be designed in order to get the specified gain/noise figure?
- Will it fit in the cubesat dimensions?
- Is the power usage within the boundaries?

1.2 Outline

The outline of this thesis is as follows. Specifications are presented in Chapter 2, the way these specifications are determined is by system calculations of the front end. The system calculations are based on a combined assumption about the antenna, the ADC and a certain topology. After that a design is presented, which is then simulated in Chapter 3. Chapter 3 also contains simulations of the antenna feed gap size. The thesis finishes with conclusions and recommendations.

Chapter 2

Design & Theory

In this chapter, the design process for the front end is examined. The front end consists of an antenna, a receiver architecture and a conversion to the digital domain. First the existing antenna is examined and optimised for maximum performance. After that, the system calculations are done to determine what the receiver architecture should look like. Following the system calculations, an Analog to Digital Converter (ADC) is chosen. Once that is all known the receiver architecture can be designed in detail. A schematic overview of the front end is shown in Figure 2.1.

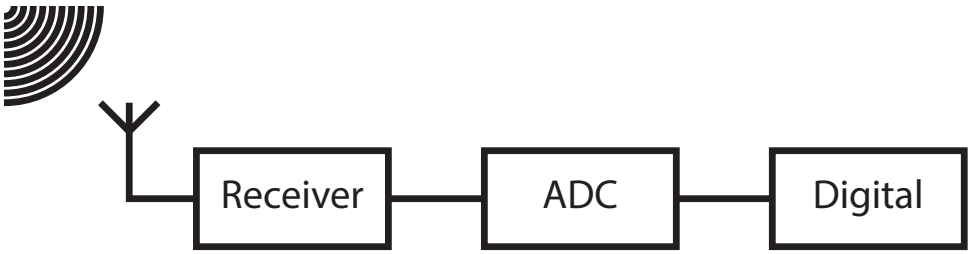

Figure 2.1: Overview of the total front end with antenna.

2.1 Specifications

The specifications are determined using a combination of the OLFAR main specification and the system calculations done in Section 2.4. The OLFAR specifications are presented in the document 'OLFAR Straw man design' [13]. For this thesis the important OLFAR specifications are given in Table 2.1

Table 2.1: Specifications for OLFAR.

Name	Parameter	Specified value
OF1	Frequency	0.3 to 30 MHz
OF2	Instantaneous Bandwidth	10 MHz
OF3	Spectral Resolution	1 MHz
OF4	Node dimensions	10x10x30 cm
OF5	Number of nodes	10 initially, 50 eventually
OF6	Baseline	$\sim$ 100 km

For the astronomical receiver unit (ARU) the specifications are presented in Table 2.2. The specifications are derived using assumptions about the antennas and the analog to digital converter at the end of the signal chain. The details of the determination of the specifications are elaborated in Section 2.4.

The power requirements of a OLFAR node are not yet well defined. The straw man design of OLFAR states that the potential 6 ADC's on board of the OLFAR node are allowed to consume a maximum of 2 [W]. And the receiver payload is allowed to spend 2.5 [W] [13].

Table 2.2: Specifications the astronomical receiver unit (ARU).

Name	Parameter	Specified value
AS1	Frequency	0,3 to 30 [MHz]
AS2	Voltage gain	90 [dB]
AS3	Noise Figure	18-8 [dB]
AS4	Maximum size requirements	10x10 [cm]
AS5	Power Usage (receiver)	2.5 [W]
AS6	Power Usage (ADC)	2 [W]
AS7	Number of antennas	3
AS8	Interference requirement	Robust

2.2 Antenna

The antenna needed for the receiver is the 'Smart Antenna System (SAS)' proposed by K. A. Quillien in [11]. This unit consists of three Triangular Retractable and Collapsible (TRAC) monopole antennas, and a certain deployment mechanism. The tunable parameters of this antenna are the length and the thickness of the antenna. The most important parameter to choose is the length, which directly influences the resonant behaviour of the antenna [14].

Once the physical dimensions of the antenna are known, a model for this antenna can be created that is needed for the system calculations (see Section 2.4).

2.2.1 Previous Work

The TRAC antenna was designed for its compactness while still retaining its stiffness. This means that the deployed antennas are relatively straight [11]. An OLFAR node will eventually contain two of these modules on each side of the satellite. These two modules will form two sets of three orthogonal monopoles with the option to use them as dipoles. The length of the antennas has to be predetermined and cannot be adjusted in orbit, because the antenna has to be fully deployed in order to keep the configuration. A photo of the completed SAS is presented in Figure 2.2 [11].

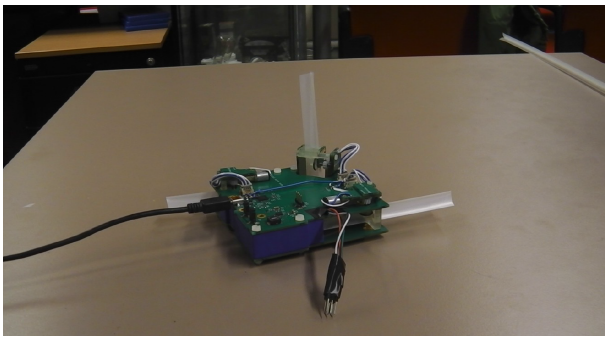

Figure 2.2: Photo of the Smart Antenna System module.

2.2.2 TRAC Antenna

A TRAC antenna consists of a rolled up length of polymer that is pushed out of a slot. As soon as the polymer exits this slot it unfolds into a 'Y' shape. In the middle of this shape a conductor is placed which will form the antenna. One SAS forms three antennas arranged in one dipole with a perpendicular monopole. A schematic view of this antenna can be seen in Figure 2.3.
The parameters in the figure are:

- w width of the support structure.
- t thickness of the conductor
- l length of the antenna

It should be noted that there are limitations when considering these antenna elements as ideal dipoles or monopoles. Firstly, for the dipole configuration, the feed gap size is quite large, especially when the dipole is connected across the length of the satellite (feed gap size spanning the length of the satellite which is about 30 cm). When considering monopoles, the ground plane is very small (the surface of the satellite). The significance of the influence of these configurations is examined in Section 2.2.8.

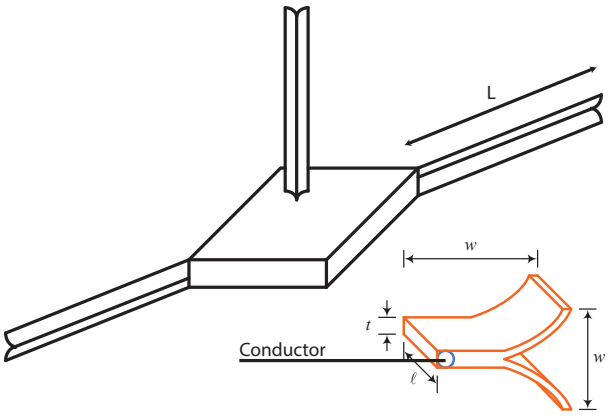

Figure 2.3: Schematic impression of the SAS.

2.2.3 Thickness of the antenna conductor

The thickness of the antenna influences the loss resistance and the bandwidth. It also has influence on the reactance of the antenna [14]. An important parameter for the antenna is the loss resistance which is purely determined by the imperfect conductivity of the antenna. Although it is unknown which types of conductors can be used for this antenna, the current choice is copper, but other materials are also examined [11].

Due to the frequency range of the antenna, it is expected that the skin effect plays an important role for the resistance characteristic. The low frequency resistance R_{lf}, excluding skin effect, is given by [15]:

$$R_{lf} = \frac{1}{\sigma \pi t_w^2} \cdot L \tag{2.1}$$

Where:

- σ is the electrical conductivity of the material [S/m]
- t_w is the radius of the wire [m]
- L is length of the wire [m]

The frequency dependent component of the loss resistance is given by:

$$R_{hf} = \frac{1}{\sigma(\pi t_w^2 - \pi(t_w - \delta)^2)} \tag{2.2}$$

Where:

- t_w is the radius of the wire [m]
- σ is the conductivity of the material [S/m]
- δ is the skin depth in [m]

The skin depth is determined by the following expression:

$$\delta = \frac{1}{\sqrt{\pi f \mu_0 \sigma}} \tag{2.3}$$

Where:

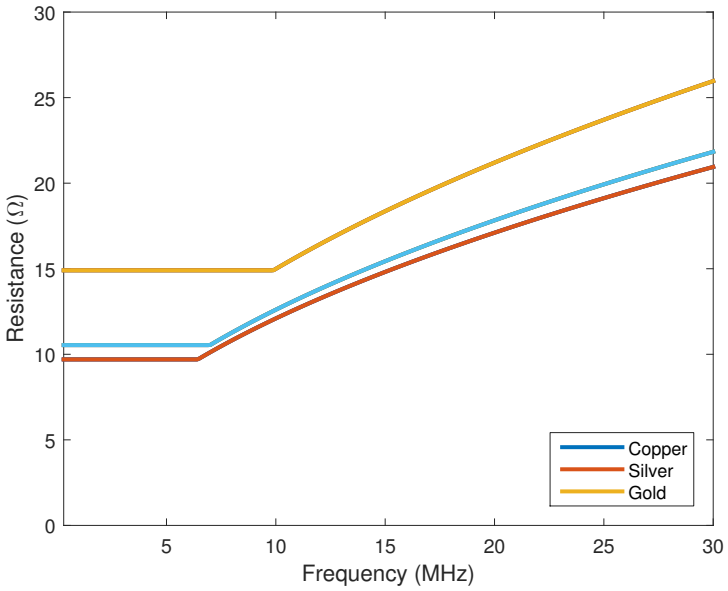

Figure 2.4: Loss resistance of the antenna versus frequency

- f is the frequency in [Hz]
- μ_0 is the electromagnetic permeability [$\mathrm{H} \cdot \mathrm{m}^{-1}$]
- σ is the conductivity of the material [S/m]

The frequency dependant loss resistance can then be determined over a frequency range. The loss resistance for the band of interest for a 9.6 m dipole is shown in Figure 2.4.
It is ideal to keep the loss resistance as low as possible in order to keep the thermal noise as low as possible. A lower loss resistance also increases the efficiency of the antenna. Therefore, the thickness of the antenna conductor is chosen as thick as possible for this SAS [11]. The resulting thickness of the conductor is then **0.2 mm**.

2.2.4 Length of the antenna

The length of the antenna influences a lot of parameters of the SAS. The important parameters that are influenced are:

- Beamwidth
- Impedance
- Frequency characteristic across the band
- Intrinsic cross polarisation ratio (IXR) [16]
- Resonant frequency

For a half-wave dipole it is important to know that there are two important resonance frequencies. The half-wave resonance and the full-wave resonance. At the full-wave resonance, the impedance will become 'infinite'. Below the half-wave resonance, the antenna will behave capacitively. A paper by D.M.P. Smith [12] did a comparative study for the antenna configurations for this particular antenna and came to the conclusion that the ideal length of the antenna is 4.8 m per monopole (forming 9.6 m dipoles in dipole configuration). The study also suggests that the placement of the monopoles does not influence the performance of the instrument. Also, the change in beam width is not an issue.

2.2.5 Impedance

In order to obtain a model for the antenna the impedance of the antenna has to be determined. The antennas are modelled as 0.2 mm thick dipoles with a length of 9.6 meters. The impedance of the antenna consists of a loss resistance (R_{loss}), a radiation resistance (R_{rad}) and a reactance (X_{ant}). The loss resistance for this antenna has been determined in Section 2.2.3. The antenna resistance is given by [14]:

$$R_{rad} = \frac{\eta}{2\pi}\Big[C + ln(kl) - C_i(kl) + \frac{1}{2}sin(kl)[S_i(2kl) - 2S_i(kl)] + \frac{1}{2}cos(kl)[C + ln(kl/2) + C_i(2kl) - 2Ci(kl)\Big] \tag{2.4}$$

And the antenna reactance is given by [14]:

$$X_{ant} = \frac{\eta}{4\pi}\Big[2S_i(kl) + cos(kl)[2S_i(kl) - S_i(2kl)] - sin(kl)\big[2C_i(kl) - C_i(2kl) - C_i\big(\frac{2ka^2}{l}\big)\big]\Big] \tag{2.5}$$

Where:

- η the wave impedance of a wave in free space
- C constant equal to $C = 0.772$
- k is the wave number equal to $\frac{2\cdot\pi}{\lambda}$
- l is the length of the antenna [m]
- C_i is a cosine integral defined by: $C_i(x) = -\int_x^\infty \frac{cos(t)}{t}dt$
- S_i is a sine integral defined by: $S_i(x) = \int_0^x \frac{sin(t)}{t}dt$
- a is the diameter of the antenna conductor [m]

Then the input radiation resistance and the input reactance of a lossless dipole can be determined by using:

$$Rin = \frac{R_m}{sin(\frac{kl}{2})^2} \tag{2.6}$$

$$Xin = \frac{X_m}{sin(\frac{kl}{2})^2} \tag{2.7}$$

The reactance and radiation resistance with respect to frequency for two different dipoles can be seen in Figure 2.5 & 2.6. The 9.6 meter dipole is half wave resonant in the middle of the band, and the 4.8 meter dipole is considered a short antenna. It is shown that the short antenna behaves more like a capacitance over the whole band, and the resonant antenna shows a more fluctuating impedance profile.

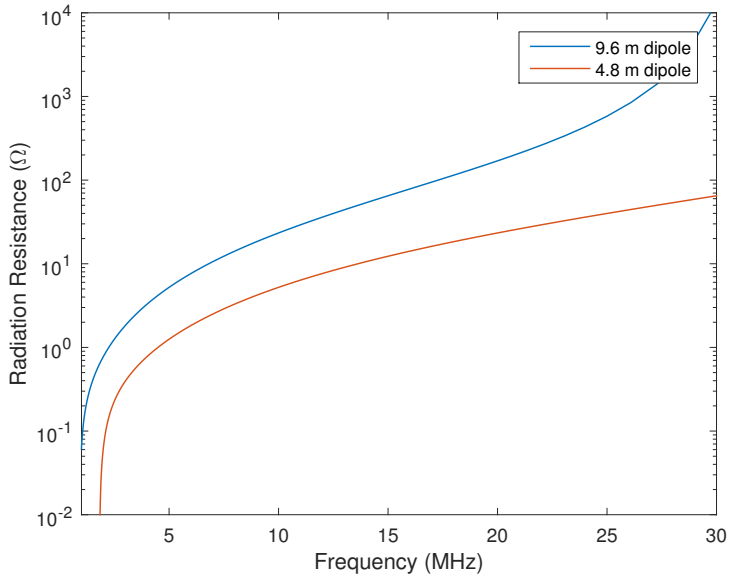

Figure 2.5: Radiation resistance as a function of frequency for a 9.6 m and a 4.8 m dipole.

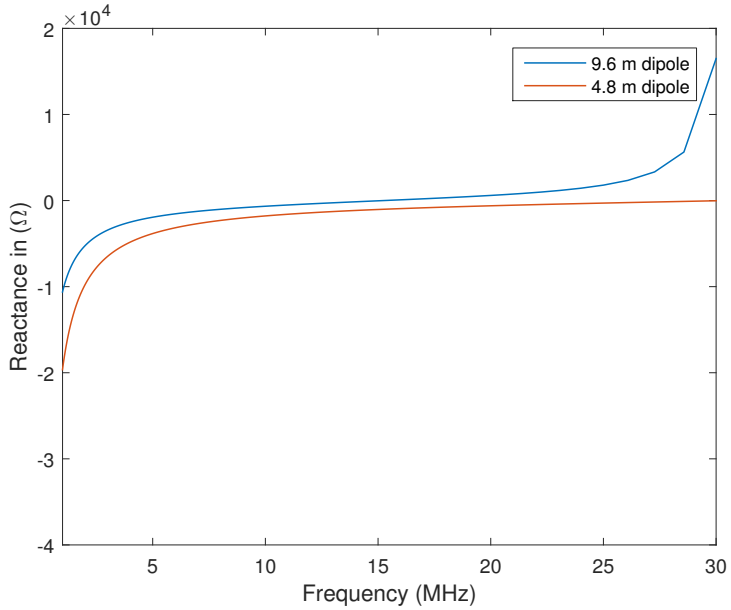

Figure 2.6: Antenna reactance as a function of frequency for a 9.6 m and a 4.8 m dipole.

2.2.6 Model

After the different components of the antenna have been calculated, a suitable circuit model is created. The circuit model is given in Figure 2.7. As stated before, the model consists of a loss resistance, a radiation resistance, a reactance and a load impedance. Moreover the model includes a voltage source used to model the signal produced by the received electric field.

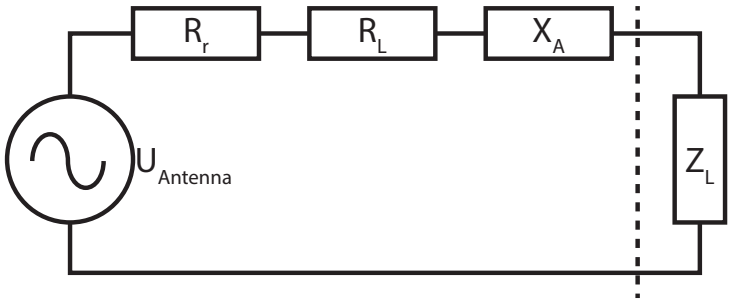

Figure 2.7: Equivalent circuit model of the antenna.

2.2.7 Beamwidth

The beamwidth of the antenna is important for the performance of the ARU. Because the orientation of each satellite is difficult to control, it is necessary to get a near omni-directional sensitivity pattern for each node (using three orthogonal dipoles). The drawback of having longer antennas is that the half power beam width (HPBW) of each dipole is decreased at antenna lengths close to a wavelength. The difference in half power beam width between different antenna length for an infinitesimal dipole is presented in Figure 2.8. Here it is shown that different lengths of antennas (expressed in amount of wavelengths) have different beampatterns. The HPBW is listed for every length of antenna.

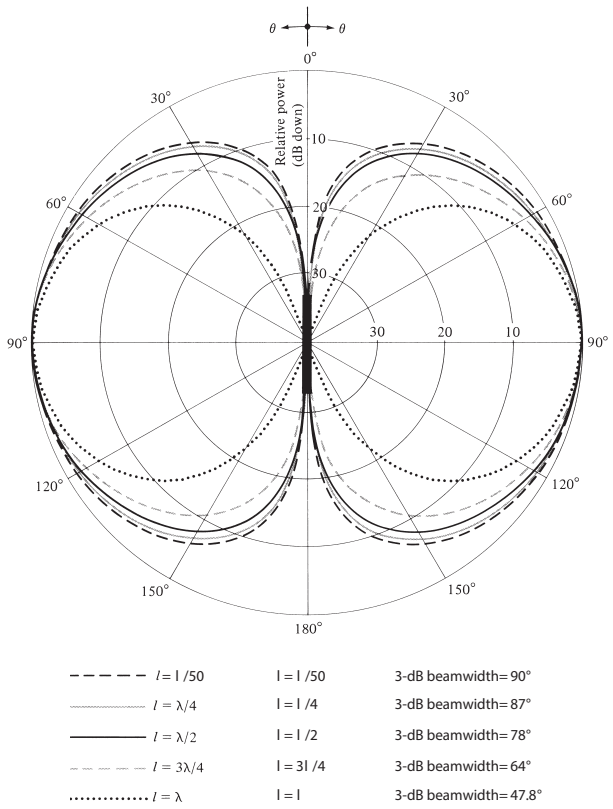

Figure 2.8: Beampattern for different antenna lengths for a sinusoidial current distribution. [14]

However the study done by D.M.P Smith et al. in [12] shows that this resulting decrease in beamwidth is acceptable with the OLFAR system.

2.2.8 Limitations

The presented dipoles and monopoles are not perfect in any way. There are a few drawbacks to this design:

Dipole configuration

When connecting the antennas in a dipole configuration the main issue is that there is not an infinitesimal feed gap. A non infinitesimal feed gap influences the current distribution across the wire [14]. How much influence this has on the characteristics of the antenna is researched by performing simulations for different feedback sizes. The results of these simulations will be presented in Section 3.1. From these simulations it was clear that the influence of the feed gap is negligible and that the model for a dipole with an infinitesimal feed gap is a suitable model for designing the amplifier.

Monopole configuration

For the monopole configuration, the drawback is that there is not a infinite ground plane. The effect of having only a small satellite as a ground plane has also been examined in the paper of David Smith, and the effect can be neglected [12].

2.2.9 Intrinsic Cross Polarisation Ratio & Aperture

Two important factors for radio astronomy are to get an aperture as large as possible, as well as a good separation between polarisations received [17] [12]. The measure of the leakage of one polarisation to another is called the intrinsic cross polarisation ratio(IXR). Research has been done by ASTRON regarding the IXR of the antennas discussed in this section [12]. This paper discusses the advantageous IXR when using longer antennas, and concludes that longer antennas are beneficial for the IXR.

Another advantage of using longer antennas is that the aperture is larger across the frequency band. The maximum effective aperture of a dipole is given by:

$$A_{eff} = \frac{\lambda^2}{4\pi} D_0 \tag{2.8}$$

This expression shows that a resonant dipole will have a larger effective aperture, due to its increased maximum directivity (D_0) [14].

2.2.10 Final Configuration

For the final configuration there are three feasible options, displayed in Figure 2.9. Each configuration shows the configuration of the monopoles (M) and/or dipoles (D).
In order to choose a final configuration it is important to consider the following considerations:

I Total amount of ADCs channels required (2 modules)

II Each node has two identical ARUs (+), every node needs two different ARUs (-)

III There is no electrical connection between the monopoles across the length of the satellite(+)/ there is an electrical connection required(-)

IV Power consumption of the module

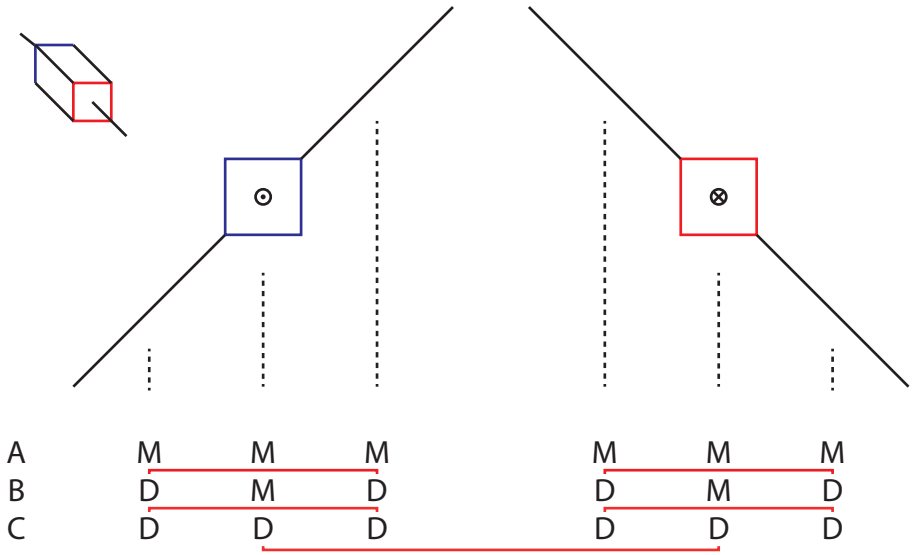

Figure 2.9: Three different configurations of the monopole antennas.

Table 2.3: Comparison between different setups.

Configuration	I	II	III	IV
A	6	+	+	+/-
B	4	+	+	+
C	3	-	-	++

These parameters are summarized in Table 2.3.
The final configuration that is chosen is the use of one dipole and combine the monopoles across the span of the satellite (configuration C). The main reason for this is that a single monopole does not have a appropriate ground plane. And this will heavily affect the beam pattern. The beam pattern will be most useful when both monopoles will be combined. This also means that one ADC channel can be used.

2.3 Topologies

The system calculations in Section 2.4 give the specifications with which the receiver has to comply with. There are two ways of making this receiver. One topology involves frequency translations and filters called the selective band topology. The other uses the entire band available. The different topologies are analysed and then a choice of topology is made.

An important parameter when considering both topologies is also the instantaneous bandwidth. This is the bandwidth which can be observed at the same time. When a selective band topology is chosen not the whole band can be sampled instantaneously.

2.3.1 Wideband

The wideband topology simply consists of an amplifier with a bandpass filter and an ADC. The amplifier amplifies the sky noise temperature to required signal levels suitable for the ADC. The bandpass filter will function as a pre-sampling filter as well as to band-limit the signal to the required band. A drawback of this design is that the required ADC has to be very powerful due to the high bandwidth (and thus high sample rate). This also means that the data rate and the power consumption of the receiver will increase [18].

An advantage is the amount of flexibility that is obtained in return. Since the whole signal band is digitised, the reconfigurability is all in the digital part of OLFAR (e.g. digital filters and digital signal conditioning), and thus, easy to adjust. This means that, in orbit, the receiver digital architecture can be adjusted.

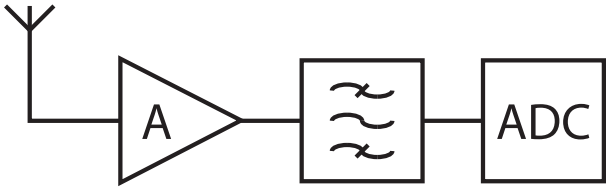

Figure 2.10: Schematic overview of the wideband topology.

2.3.2 Selective Band

The main purpose of the selective band topology is to reduce the instantaneous bandwidth. The topology consists of a mixer with a tunable local oscillator so that the frequency band can be translated to a intermediate frequency. On a standardised intermediate frequency it is easy to get a sharp Surface Acoustic Wave (SAW) filter. After this filter, the selected band is then translated back to baseband. This bandwidth reduction also means that the ADC is allowed to be 30 times slower, dissipating less power than the high sample rate ADC [18]. Another advantage is that it feeds less data to the Digital Signal Processor (DSP).

There are several disadvantages to this topology. First of all, there are more components needed to realise this topology. Secondly, the instantaneous bandwidth is limited to the bandwidth of the SAW filter. There are also more components which can introduce non-linearities.

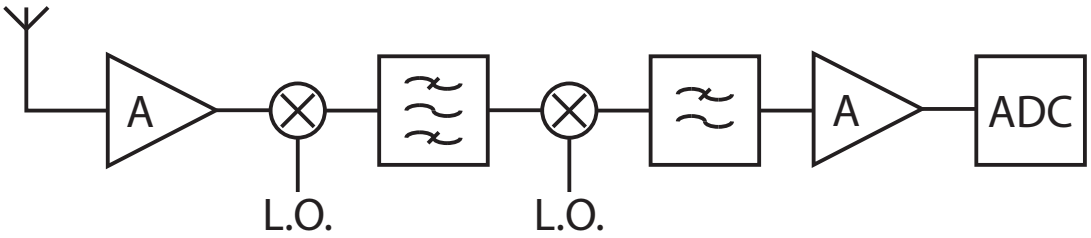

Figure 2.11: Schematic overview of the selective band topology.

2.3.3 Balun

When using dipoles, a balun is required to convert the differential ended signal into single ended. In this case, the balun can be placed either right after the antenna, or after the amplifier (the so called active balun). The advantage of an active balun is that the noise contribution of the balun is severely reduced. However, because of variances in the both signal chains, the signal might be degraded slightly.

2.4 System Calculations

Specifications of a receiver are usually determined by examining the expected input signal and required output signal of a system.

For a radio astronomy receiver, this is quite difficult since the signals are unknown and expected to be very weak. This makes determining suitable specifications a difficult task. The back-end specifications /implementation for OLFAR are still unknown. The one thing that is known is that the signal has to be digitised and digitally [8]. The ADC is not yet chosen, so depending on the implementations selected in Section 2.3 a suitable ADC can be determined. Based on the ADC, the system specifications can be determined through system calculations. The exact system calculations are explained in this Section.

The Matlab code for the system calculations is presented in Appendix A.1.

2.4.1 Astronomical Signal

The eventual science will be done using interferometry with the OLFAR cluster. Hence the required input signal received at the antenna is ambiguously defined. Therefore astronomers usually dimension the receiver input signal with respect to the received sky noise. This sky noise is the noise present due to galactic background radiation [17]. There has only been one measurement done of the sky noise in space [19]. Therefore an empirical model of the DARIS study has been used [7]. This model can predict the sky noise for certain frequencies. The expression for the galactic sky noise temperature is:

$$T_{sky}(f) = T_{1k} \cdot \left\{ \left(\frac{c}{f \cdot l_0} \right)^{2.55} + \left(\frac{f}{f_0} \right)^{1.8} \right\} + T_{bg}$$

Where:

- T_{1k} is a constant equal to 1 [K]
- l_0 is a constant equal to 0.2008 [m]
- f_0 is a constant equal to 10 [GHz]

- T_{bg} is a constant equal to 2.7 [K]
- f is frequency [Hz]
- c is speed of light in [m/s]

The sky noise from 0.3 to 30 MHz is shown in Figure 2.12.

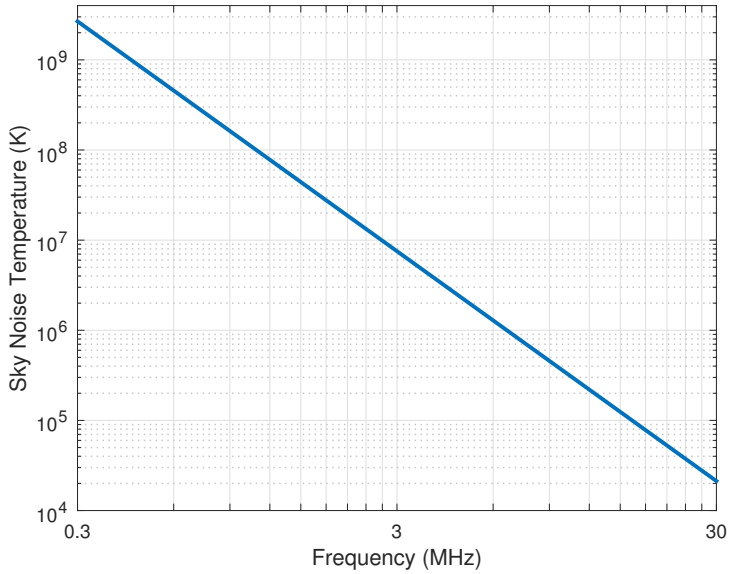

Figure 2.12: Sky noise from 0.3 to 30 MHz.

Antenna Noise Temperature

The sky noise received at the clamps of the antenna will depend on the efficiency of the antenna and the amount of available sky-noise on a certain frequency. The relationship between the sky noise at the clamps of the antenna is given by [17]:

$$T_{ant} = e_0 \cdot T_{sky} + (1 - e_0) \cdot T_{phys} \tag{2.9}$$

Where:

- e_0 is given by the total efficiency of the antenna.
- T_{sky} is the sky noise temperature of the antenna [K].
- T_{phys} is the physical temperature of the antenna [K].

The efficiency of the antenna consists of two parts. The first part is the conduction- dielectric efficiency e_{cd}. The second part is the reflection efficiency between the antenna itself and the load e_r. The conduction and dielectric efficiency is given by [14]:

$$e_{cd} = \left| \frac{R_{rad}}{R_{rad} + R_L} \right| \tag{2.10}$$

Where:

- R_{rad} is the radiation efficiency [Ω].
- R_L is the loss resistance [Ω].

The reflection efficiency e_r is given by:

$$e_r = (1 - |\Gamma|^2) \tag{2.11}$$

$$\Gamma = \left| \frac{Z_{ant} - Z_L}{Z_{ant} - Z_L} \right| \tag{2.12}$$

Where:

- Γ is the reflection coefficient between the antenna and the load.
- Z_{ant} is the impedance of the antenna [Ω].
- Z_L is the impedance of the antenna [Ω].

Both efficiencies are shown in Figure 2.13 for the frequency range of 0.3 to 30 MHz. The efficiencies are calculated using a termination resistor of 1800 [Ω], because it is a good trade-off between permissible noise figure and matching.

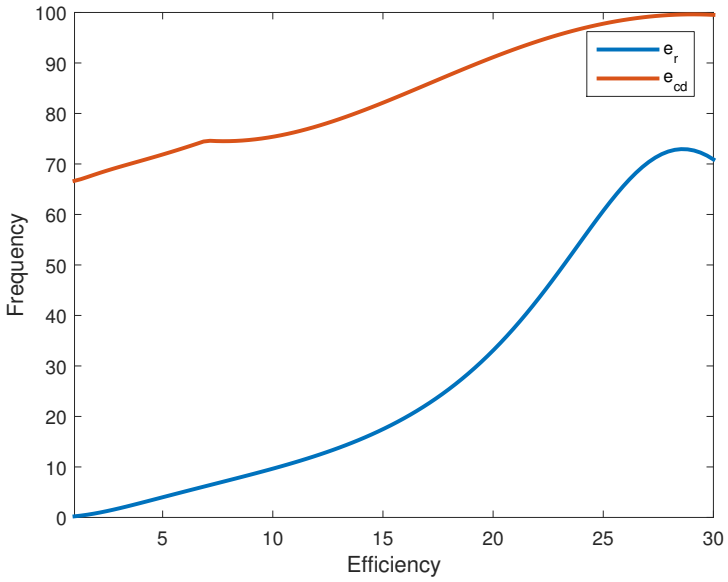

Figure 2.13: The reflection efficiency (e_r) and the antenna

Using these efficiencies the antenna sky noise temperature can be determined. The Antenna noise temperature is presented in Figure 2.14.
The input sky noise power put into the amplifier can then be calculated by integrating the sky noise power over the bandwidth and multiplying it by the Boltzmann constant. With a load impedance of 1.8 [$k\Omega$], the input signal voltage can then be determined by:

$$P_{sky|in} = T_{ant} \cdot B \cdot k \tag{2.13}$$

$$V_{sky|in} = \sqrt{P_{sky|in} \cdot Z_L} \tag{2.14}$$

$$V_{sky|in} = 2.7314 \cdot 10^{-5} V \tag{2.15}$$

Permissible Noise Figure

The noise requirement for the system is determined by a rule of thumb used in astronomy. This rule is that the system has to be sky noise limited. A sky noise limited system typically is defined as a system which is not allowed to contribute more than 1/10th of the available sky

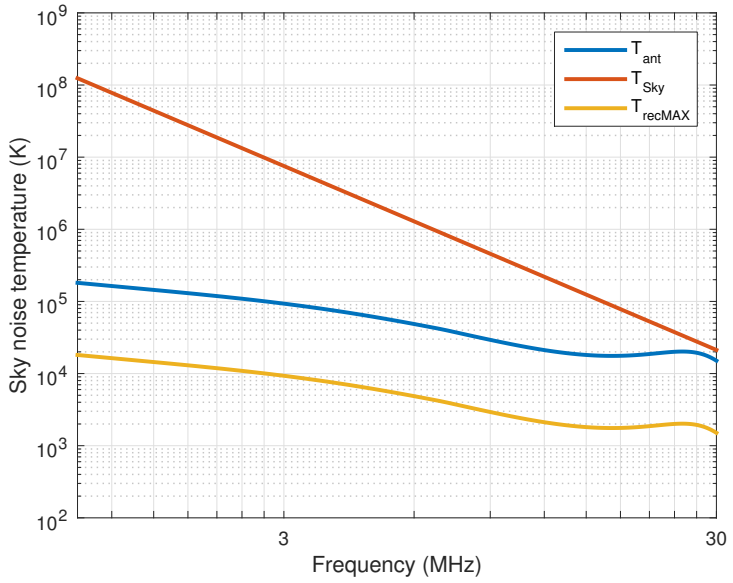

Figure 2.14: Antenna sky noise temperature

noise to the system. This is equal to the equivalent noise temperature of the system, hence the maximum noise figure can be calculated with the following expression [20]

$$NF = 1 + \frac{T_e}{T_0}$$

The system equivalent noise temperature is the amount of noise the amplifier and the ADC can contribute. The noise temperature of the ADC can be determined by looking at the specifications of a certain selected ADC.

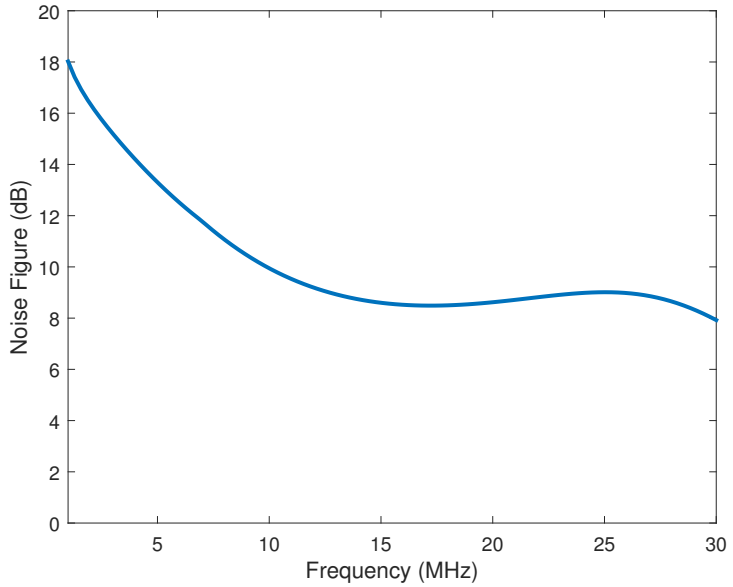

Figure 2.15: Permissible noise figure over the frequency range

2.4.2 AD Converter

An important factor in the receiver design is what signal is needed for the ADC. The ADC will be the last analog step for the receiver. The input signal has to be conditioned appropriately to enter the ADC. The type used is the LTC2158-14 made by the company Linear Technology. This ADC is chosen because it has a sample rate high enough to sample the entire band sufficiently. Another advantage is that it is cheap, and has good noise performance, and high Spurious Free Dynamic Range (SFDR). The specifications of this ADC can be derived from the data sheet. The important specifications for this chip are presented in Table 2.4.

Table 2.4: Specifications the analog to digital converter.

Parameter	Specified value
Data rate	310 Mbps/2 channels
Input voltage	1 Vpp
Input Impedance	10 [kΩ]
SFDR	88 dB
Noise temperature	505 [K]
Power consumption	725 mW

Third order intercept point and compression point do not have any significance when dealing with ADCs [21]. This is because the ADC will go into hard compression when the input power is exceeded (as depicted in Figure 2.16). Thus the signal at the input of the ADC must remain below the maximum allowable input signal.

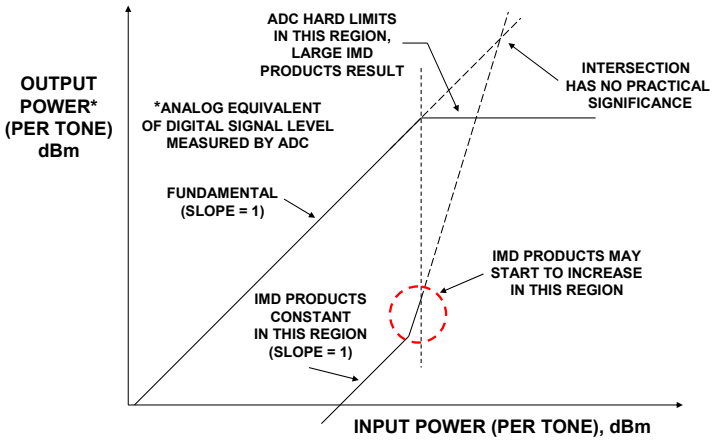

Figure 2.16: Compression point and non-linearities in ADCs [21]

2.4.3 Receiver

For the total receiver calculations, the required input signal needs to be considered. It is undesirable that the ADC clips. The input required input signal is chosen below the maximum input voltage of the ADC to give some room before the ADC will clip. The maximum input signal for this given ADC is 1.32 Vpp. In order to give some headroom the required input signal is dimensioned on 1 Vpp.

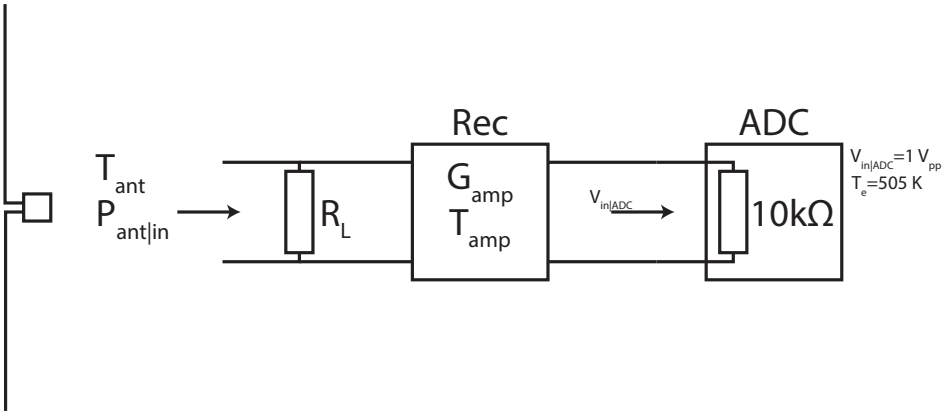

Figure 2.17: Topology of the receiver

The equivalent noise temperature of the system is given by a combination of the amplifier noise temperature and the ADC noise temperature combined with the gain of the amplifier (Equation 2.16).

$$T_e = T_{amp} + \frac{T_{ADC}}{G_{amp}} \tag{2.16}$$

$$\frac{1}{10}T_{ant} = T_{amp} + \frac{T_{ADC}}{G_{amp}} \tag{2.17}$$

$$\tag{2.18}$$

Since the required input signal is known for the ADC, the gain can be determined by determining the input voltage coming from the antenna. The input voltage can be derived by using the antenna noise temperature (see Equations 2.19 to 2.21).

$$G_{amp} = 20 \cdot^{10} \log\left(\frac{V_{in|ADC}}{V_{in|ant}}\right) \tag{2.19}$$

$$V_{in|ant} = \sqrt{(k \cdot T_{ant} \cdot B) \cdot Z_L} \tag{2.20}$$

$$G_{amp} = 91dB \tag{2.21}$$

The maximum noise power at the input of the ADCis calculated as follows:

$$P_{N|ADC} = k \cdot B \cdot (0.1 \cdot T_{ant} \cdot G_{amp} + T_{ADC}) \tag{2.22}$$

The signal voltage has been dimensioned on 1 V_{pp} so the signal power is:

$$P_{S|ADC} = \frac{\left(\frac{V_{ADC|pp}}{\sqrt{2}}\right)^2}{Z_{ADC}} \tag{2.23}$$

This gives a worst case signal to noise ratio of 10 dB.

Table 2.5: Specifications derived from system calculations.

Parameter	value
Frequency	0.3 to 30 MHz
$V_{in\|ant}$	$2.7314 \cdot 10^{-5}$ [V]
$V_{in\|ADC}$	1 [V]
G_{amp}	91 [dBV]
SNR	10 [dB]
Effective number of bits ($ENOB$)	$\sim$ 1.4 [bits]
Z_L	1000 [Ω]

2.5 Design

For the design of the receiver, the wideband topology is chosen. The reason to use this topology is mainly due to the large instantaneous bandwidth. Another advantage is that with digital signal processing flexibility can be added, for example by implementing filters. This topology basically consists of an amplifier and a bandpass filter. The realisation of an amplifier, different types can be chosen. First the type of amplifier is chosen, followed by the technology. After this, a design can be made which will form the entire amplifier.

2.5.1 Overview

When choosing an amplifier type, certain aspects need to be taken into consideration. First of all, the input impedance is important since this directly influences on the reflection coefficient. Secondly, the noise contribution is very important because of the strict noise requirements. Thirdly, the required components for setting the gain/biasing. Three types of amplifiers are considered. The first one is the non-inverting voltage amplifier. The second one is the inverting voltage amplifier. And the last one is the charge amplifier. In Table 2.6 the types of amplifiers are compared. The different type of amplifiers are presented in Figure 2.18

Table 2.6: Comparison between different amplifiers.

Property	Non-inverting	Inverting	Charge
Gain	$1+\frac{R_f}{R_1}$	$-\frac{R_f}{R_1}$	$-Rf$
Noise	-/+	+	+
Input Impedance	High	Low	Low

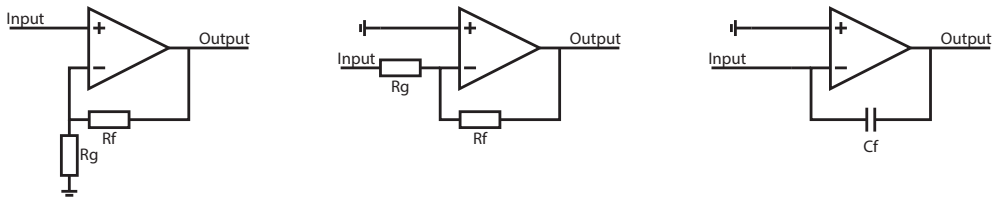

(a) Non inverting amplifier (b) Inverting amplifier (c) Charge amplifier

Figure 2.18: Different type of amplifiers

Because the non-inverting topology allows for a high input impedance, and a reasonable noise performance, this topology is chosen. The amplifier will be realised by using a low-noise operational amplifier (opamp) to keep the noise contribution to a minimum. The advantage of using an op amp compared to a transistor device is the massive amounts of gain a single stage can

bring as well as ease of implementation. Because of the low number of units produced, the costs of the component will not matter too much. Another advantage why opamps are a favourable choice are the power supply rejection ratio and common mode rejection ratio which make them quite immune to interference.

2.5.2 Static protection

Static protection is needed because large static charges build up on the large antennas in space. The best solution is to have something that doesn't interfere with the signal. The first one is to use a series of DC blocking capacitors, so the DC from the outside doesn't destroy the amplifier. Another option is to use gas discharge tubes to breakdown high static voltages while leaving the signal untouched. A disadvantage of gas discharge tubes though is that the they are more bulky than capacitors, so it might take up a lot of usable space.

2.5.3 Matching

Because of the capacitive nature of the source impedance, (see Section 2.2.6), there are a lot of limitations with matching. The Bode-Fano criterion states the following: for a given series RC combination with a passive lossless matching network a certain reflection coefficient is obtainable for a certain bandwidth. If this bandwidth is increased, then the reflection coefficient will degrade [20]. This means that perfect matching is only obtainable for a very limited bandwidth. Since the OLFAR bandwidth is wide, the choice is made to have a larger bandwidth with a poor reflection coefficient. The Bode-Fano criterion is given by Equation 2.24. A schematic representation is given in Figure 2.19.

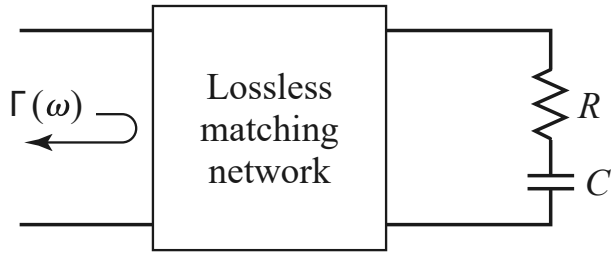

Figure 2.19: The Bode-Fano Criterion

$$\int_0^\infty \frac{1}{\omega^2} ln \frac{1}{|\Gamma(\omega)|} d\omega < \pi RC \tag{2.24}$$

More insight to the Bode-Fano criterion is given in Figure 2.20. Here two graphs with are displayed for a arbitrary RC combination. What can be seen is that a good matching for a narrow bandwidth, or a poor matching for a wide bandwidth can be chosen. From this it can be seen that the capacitance in the antenna severely limits the matching capabilities.

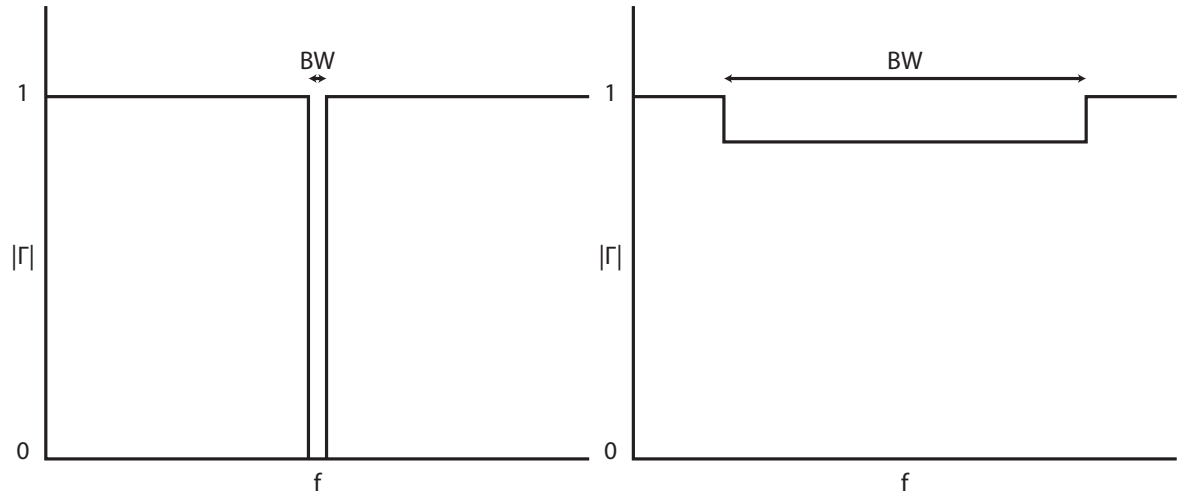

(a) Narrow bandwidth, good matching (b) Large bandwidth, poor matching

Figure 2.20: Graphical insight to the Bode-Fano criterion.

2.5.4 Gain

The required gain is high, so it is not possible to do it in one stage. The amplifier used is the LMH6624 from Texas Instruments [22]. The bandwidth used is 30 MHz, so the maximum possible gain that can be achieved by this device is determined from the gain-bandwidth (GBW) characteristic (see Figure 2.21). The maximum gain per stage is about 30 dB. So, in order to get the required 90 dB voltage gain 3 stages are needed. One thing to keep in mind is to limit the bandwidth before the ADC. This can be done by adding a capacitor in the feedback loop.

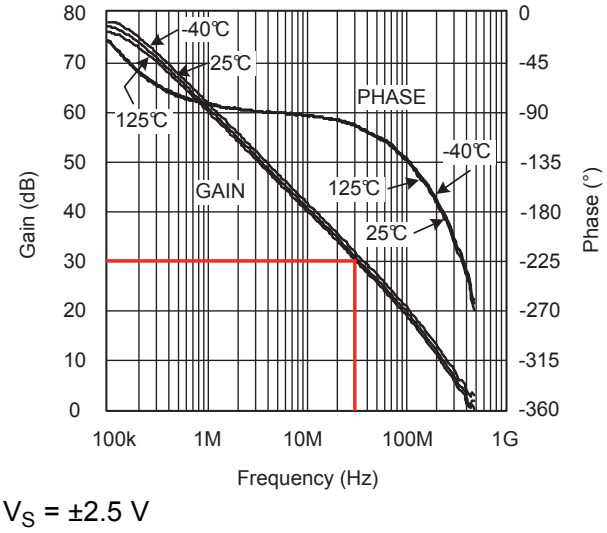

Figure 2.21: Gain bandwidth characteristic of the LMH6624

The design of one stage can be seen in Figure 2.22. This design is the aforementioned non inverting amplifier. The gain is set by resistor combination Rf/Rg. The capacitor C_{lim} limits the bandwidth of the amplifier. The gain of one stage is calculated by using equation 2.25.

$$Gain = 1 + \frac{R_F}{R_G} \tag{2.25}$$

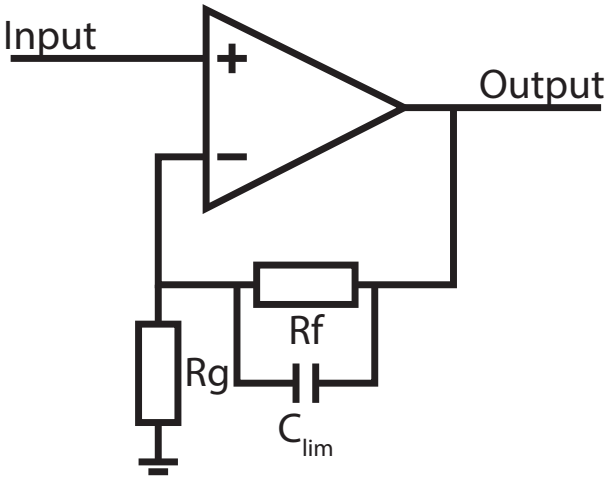

Figure 2.22: Design of one stage of the amplifier.

A possibility is to choose to use three devices subsequently and feedback to the first stage. However this option was not chosen in order to prevent high resistance values and increased noise in the system. This means however that there is a possibility that the gain may not be very precise. The eventual OLFAR system will account for this by calibrating the gain of each receiver.

2.5.5 Noise calculations

The noise calculations are done for the op amp to determine the noise figure of the first stage, since the first stage is dominant for the total noise figure of the entire system [23]. The noise of subsequent stages are divided by the first stage gain. The noise parameters of the opamp are device specific. A noisy opamp can be modeled by a noiseless opamp, an input noise voltage and an input noise current. The noise contributions of all the first stage are presented in Figure 2.23 [24].

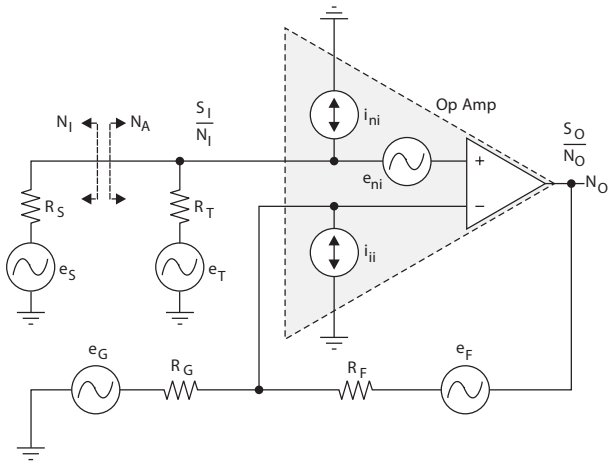

Figure 2.23: Noise contributions of a non inverting opamp. [24]

The noise figure of this system is given in by:

$$F = \frac{SNR_{in}}{SNR_{OUT}} = 1 + \frac{N_A}{N_I} \tag{2.26}$$

Here N_A is input referred noise of the device, and N_I is the noise delivered to the input of the device from the source. The noise from the source is given by Equation 2.28. The noise

generated by the device is given by 2.27.

$$N_I = 4kTR_s \cdot \left(\frac{R_T}{R_S + R_T}\right)^2 \tag{2.27}$$

$$N_A = c_1 e_{ni}^2 + c_2 i_{ni}^2 + c_3 i_{ii}^2 + c_4 e_T^2 + c_5 e_G^2 + c_6 e_F^2 \tag{2.28}$$

Where:

$$c_1 = 1 \qquad c_2 = \left(\frac{R_S R_T}{R_S + R_T}\right)^2 \tag{2.29}$$

$$c_3 = \left(\frac{R_F R_G}{R_F + R_G}\right)^2 \qquad c_4 e_T^2 = 4kTR_T\left(\frac{R_S}{R_S + R_T}\right)^2 \tag{2.30}$$

$$c_5 e_G^2 = 4kTR_G\left(\frac{R_F}{R_F + R_G}\right)^2 \qquad c_6 e_F^2 = 4kTR_F\left(\frac{R_G}{R_F + R_F}\right)^2 \tag{2.31}$$

For the single stage amplifier shown in Figure 2.23, the noise figure can be calculated as a function of frequency. The component values used in this calculation are presented in Table 2.7 This result of the calculation for the frequency range of interest is shown in Figure 2.24.

Table 2.7: Component values for the noise calculation

Component	value
R_S	Antenna impedance
R_T	1000 [Ω]
R_G	150[Ω]
R_F	4700 [Ω]
e_{ni}	0.92 [nV/$\sqrt{\text{Hz}}$]
i_{ni}/i_{ii}	2.3 [pA/$\sqrt{\text{Hz}}$]

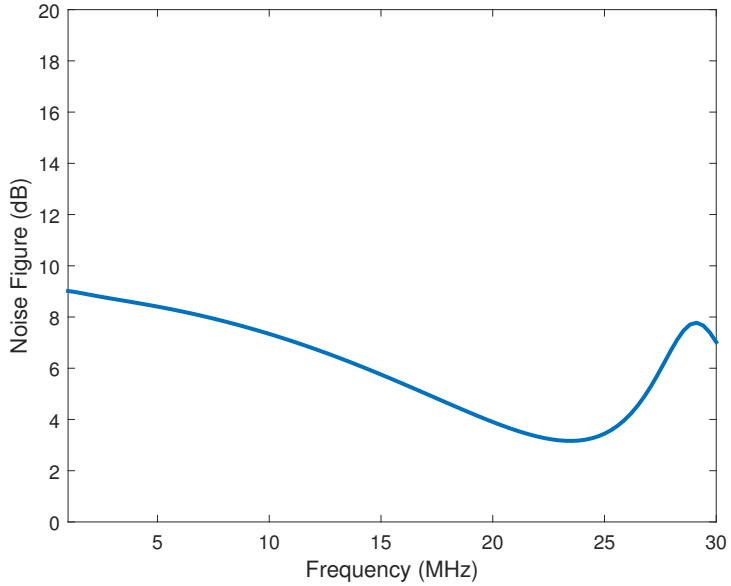

Figure 2.24: Noise figure calculations of a single stage amplifier.

The noise figure of the first stage of an amplifier chain is dominant when the gain of the first stage is high. That means that the noise figure of the first stage will largely determine the noise figure of the complete system.

The Matlab code for the calculation of the noise is presented in Appendix A.2.

2.5.6 Electromagnetic Magnetic Compatibility

In principle, the orbit of the OLFAR cluster is radio-interference free. The only interference comes from inside the node. For instance from deployment motors that deploy all the different components. It is therefore not advantageous to do astronomy measurements while the satellite is in the deployment phase. When the satellite is fully deployed, these motors can be switched off so these will not interfere on the receiver.

Other interference sources will be the different type of radios on board which will radiate on the amplifier. These do have a very different frequency and because the receiver is designed to filter only the band of interest, these radios will not cause problems. The susceptibility of the amplifier is low due to a high Power Supply Rejection Ratio (PSRR) and Common Mode Rejection Ratio (CMRR).

Conducted interference will be caused by all the digital components present in the satellite. This means that the receiver power supply needs to be filtered by capacitors.

2.5.7 Total design

The completed design of the system is presented in Figure 2.25. The total system consists of the termination resistor followed by three non-inverting amplifiers. Eventually, the signal has to enter the ADC which is the end of the front-end. The system, as depicted, is for a monopole configuration. For the dipole configuration, a balun has to be added.

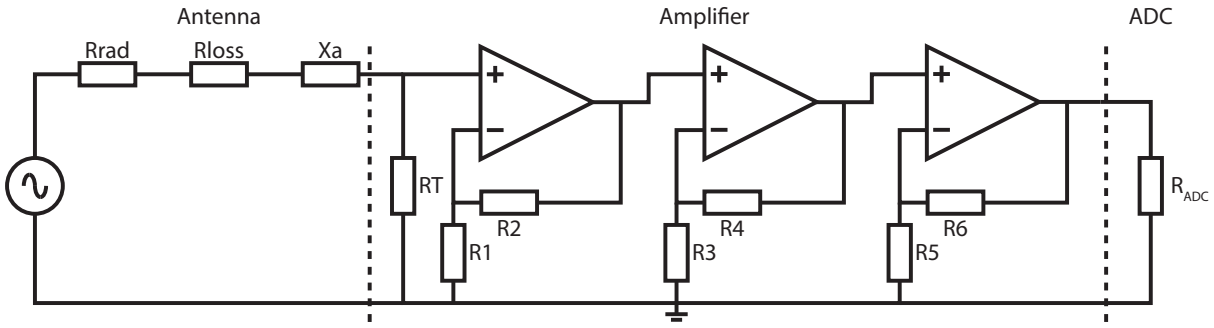

Figure 2.25: Total system design for the front-end of the OLFAR astronomy payload.

The values for all the components are given in Table 2.8.

Table 2.8: Component values for the entire front end

Component	value
R_2, R_4, R_6	4700 [Ω]
R_1, R_3, R_5	150 [Ω]
R_T	1800 [Ω]
IC1, IC2, IC3	LMH6624
ADC	LTC3269-14
Antenna	TRAC

Chapter 3

Simulations

The simulations of this thesis are two-fold. First, the antenna configuration is simulated to see if the finite feed gap has influence on the characteristics of the antenna. After the antenna parameters are all obtained, the amplifier is simulated. Antenna simulations are done by using the Ansoft High Frequency Structural Simulator, and the amplifier simulations will be done by using the Agilent Advanced Design System(ADS).

3.1 Antenna simulations

The antenna model is created by using the Ansoft Antenna Design Kit(ADK). The antenna that is created is a dipole with a diameter of 0.2 mm and a length of 9.6 m. The feed gap sizes vary from 7 cm to 35 cm, these sizes are chosen from the smallest feed gap size with steps of 5 cm to the largest. So the potential influence of a dipole made by combining opposite ends of the satellite is also considered. The used dipoles are made from copper. The following antenna parameters are simulated: antenna reactance, antenna resistance and s11 (50 Ω referred) These are the most important part on which the receiver is designed.

The Matlab code for the processing of the antenna simulation results is presented in Appendix A.3.

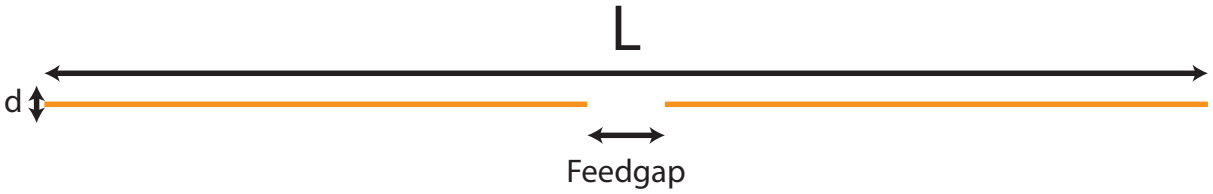

Figure 3.1: Antenna model used for simulations with HFSS.

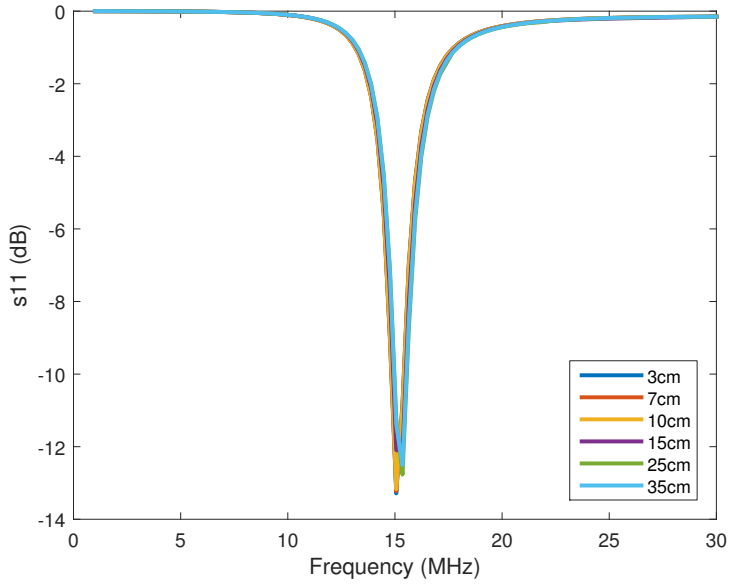

Figure 3.2: Antenna s11 (50Ω reference) for different feed gap sizes.

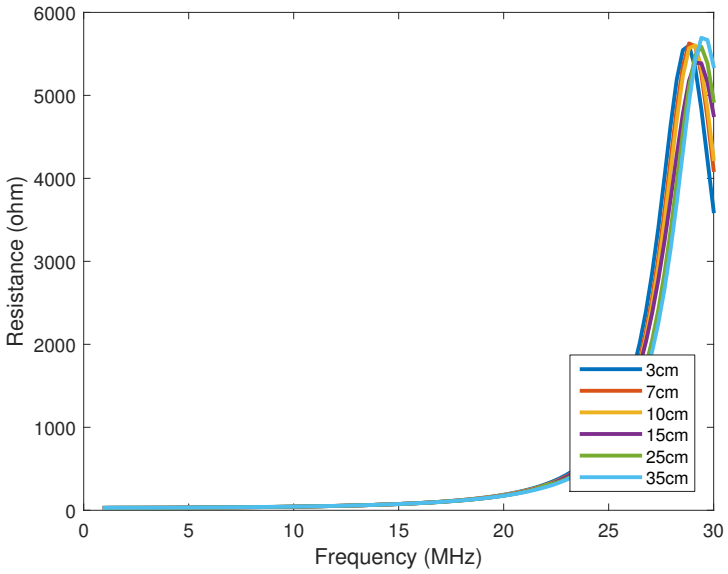

Figure 3.3: Antenna input resistance for different feed gap sizes.

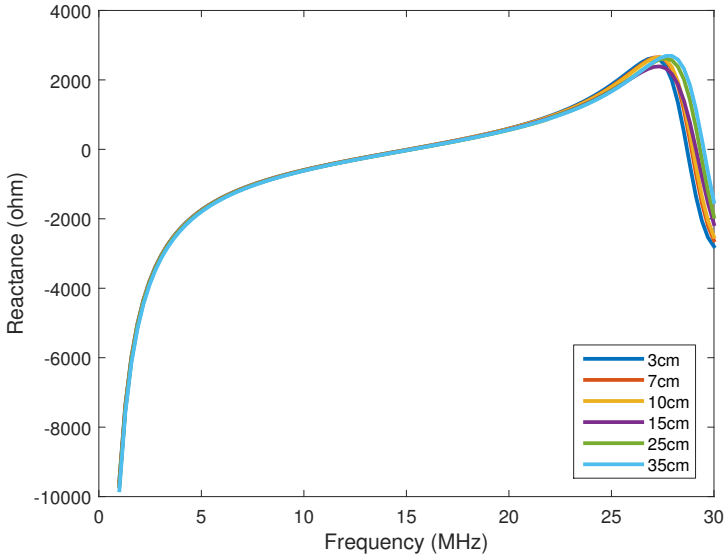

Figure 3.4: Antenna input reactance for different feed gap sizes.

3.2 Amplifier simulations

The amplifier simulations are done using ADS. The complete schematic as used in the ADS simulator can be seen in Figure 3.5. The components used in the schematic are modelled according to datasheets and simulation results obtained in Section 3.1. The opamps are modelled using the parameters obtained from the data sheet. These parameters are given in Table 3.1.

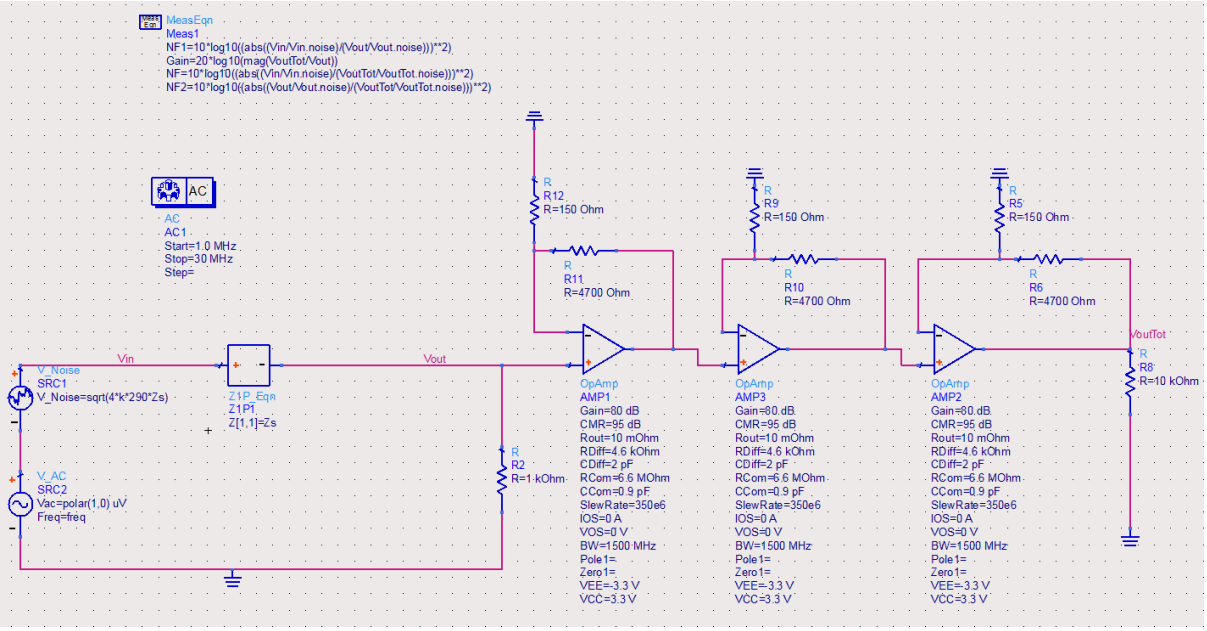

Figure 3.5: Antenna input reactance for different feed gap sizes.

Table 3.1: Opamp simulation parameters

Parameter	Value
Gain	80 [dB]
Common mode rejection ratio (CMRR)	95 [dB]
R_{out}	10[mΩ]
R_{diff}	4.6 [kΩ]
C_{diff}	2 [pF]
R_{com}	6.6 [MΩ]
C_{com}	0.9 [pF]
Slew Rate	350 [MV/s]
Bandwidth	1500 [MHz]
e_{ni}	0.92 [nV/$\sqrt{\text{Hz}}$]
i_{ni},i_{ii}	2.3 [pA/$\sqrt{\text{Hz}}$]

The source impedance is modelled by using a polynomial fit of the impedance obtained by simulating a 9.6 [m] copper dipole in HFSS. The order of the polynomial is 20 in order to obtain a reasonable fit. The noise generated by the antenna is then modelled by a noise source with a noise voltage related to the source impedance. The signal presented to the circuit is a simple sine voltage source with an amplitude of 1 μV.

The results of the gain and noise figure simulation are given in Figure 3.7 and 3.6 respectively.

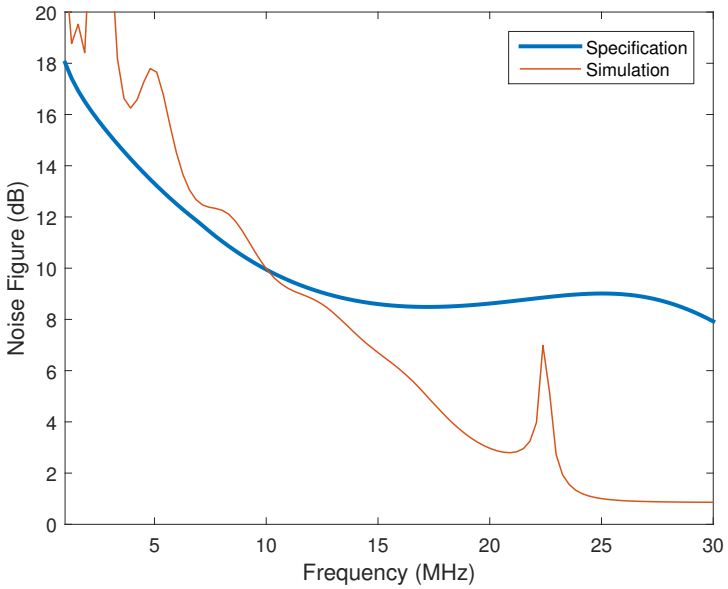

Figure 3.6: Simulated noise figure for the total amplifier.

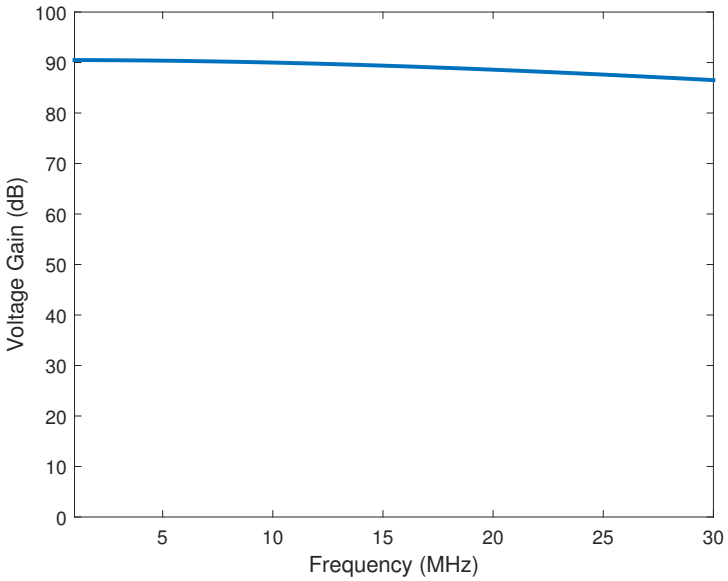

Figure 3.7: Voltage gain for the total amplifier.

The Matlab code for the processing of the amplifier simulation results is presented in Appendix A.4.

Chapter 4

Discussion & Conclusion

When all the simulations are examined, several observations can be made. First of all and the influence of the feed-gap of the antenna does not influence the antenna characteristic significantly. This means that this effect can be neglected. The antenna configuration can be used as designed. When the literature and the calculations are examined, it can be concluded that the antenna needs to be 4.8 m long and at least 0.2 mm thick (as thick as possible).

Secondly, the amplifier can be easily realised using discrete Commercial Off The Shelve (COTS) components. The resulting voltage gain is up the specified number of 90 dB. The influence of the mismatch is important, but can be managed by choosing an appropriate termination resistance. The chosen topology is simple and has a lot of advantages. First of all, a high CMRR and a high PSRR make the system very robust to interference. The favourable gain-bandwidth product means that it is easy to get the required gain in three stages. The 3 dB bandwidth lies nicely on the 30 MHz.

Most of the noise figure is below the maximum allowable noise figure for most of the band. That means that the receiver is sky-noise limited except for a small excess of noise for the lower frequencies. The amplifiers have very favourable noise characteristics so this means that the obtained noise figure is quite well across the band.

The circuit presented should also be able to fit easily on a 10x10cm PCB board used in standard cubesats. The ADC roughly has a power consumption of 0.8 W, and can serve one ARU. For both units, this comes to about 1.6 W. Meaning that this is within specification. The receiver power dissipation has not yet been determined. The specifications that are met are summarised in Figure 4.1

Table 4.1: Specifications the astronomical receiver unit (ARU).

Name	Parameter	Specified value	Conformance
AS1	Frequency	0,3 to 30 [MHz]	Yes
AS2	Voltage gain	90 [dB]	Yes
AS3	Noise Figure	18-8 [dB]	Partially
AS4	Maximum size requirements	10x10 [cm]	Not yet met
AS5	Power Usage (receiver)	2.5 [W]	-
AS6	Power Usage (ADC)	2 [W]	Yes
AS7	Number of antennas	3	Yes
AS8	Interference requirement	Robust	Not yet measured

Chapter 5

Recommendations

The first step for the completion of a complete OLFAR front-end is to build a prototype. After that, the prototype has to be measured and characterised. Once the receiver is characterised the TRAC antenna can be connected. Then the antenna can be fully tested in cooperation with the receiver front-end.

The next step is to integrate a complete PCB so the front end and TRAC-antenna become one ARU. The astronomical receiver has to integrate digital circuitry with the analogue receiver and the antenna. Furthermore the existing deploying circuit will still have to be incorporated. Once this is all done, one integrated astronomical receiver will be completed that can be controlled by the digital central processing unit of the satellite.

When the unit is integrated into the fly-ready model it is wise to test the immunity to potential interference from inside the satellite. It is recommended to integrate everything related to the ARU in one module that can be used in the cubesat standard, and makes use of the existing cubesat bus.

Bibliography

[1] R. Nijboer M. de Vos, A. W. Gunst. The lofar telescope: System architecture and signal processing. 2009.

[2] R. T. Schilizzi T. J. L. W. Lazio P. E. Dewdney, P. J. Hall. The square kilometre array. 8 August 2009.

[3] H. Falcke S. Jester. Science with a lunar low-frequency array: From the dark ages of the universe to nearby exoplanets. *New Astronomy Reviews*, 2009.

[4] M.J. Bentum S. Engelen, C.J.M. Verhoeven. Olfar, a radio telescope based on nano-satellites in moon orbit. *24th Annual AIAA/USU Conference on Small Satellites*, 2010.

[5] Kevin A. Quillien S. Engelen. The road to olfar a roadmap to interferometric long-wavelength radio astronomy using miniturized distributed space systems. 2013.

[6] Wikipedia. Radio telescope. `https://en.wikipedia.org/wiki/Radio_telescope`, 21 october 2015.

[7] R. T. Rajan M.J. Bentum F. Beli N.Saks, A.J. Boonstra.

[8] R.Noomen E. Dekens, S.Engelen. A satellite swarm for radio astronomy. *Acta Astronautica*, November 2013.

[9] M. J. Bentum J. M. Klein S. Engelen A. Budianu, A. Meijerink. Integrated downlink antennas in the deployable solar panels of a cubesat. 2014.

[10] Wikipedia. Comparison of orbital launch systems.

[11] K. A. Quillien. An astronomical antenna for olfar. 14 November 2013.

[12] Albert-Jan Boonstr Stefan J. Wijnholds David M.P. Smith, Michel J. Arts. Characterisation of astronomical antenna for space based low frequency radio telescope. 2012.

[13] Delft University University of Twente, ASTRON. Olfar straw man design. 2013.

[14] Constantine A. Balanis. *Antenna Theory: Analysis and Design, third edition.* John Wiley & Sons, Inc., 2005.

[15] Clayton R. Pauli. *Introduction to Electromagnetic Compatibility.* Wiley, 1992.

[16] Peter J. Hall Adrian T. Sutinjo. Intrinsic cross-polarization ratio of dual-linearly polarized antennas for low-frequency radio astronomy. 2013.

[17] John D. Kraus. *Radio Astronomy.* Prentice Hall, 1986.

[18] Bengt E. Jonsson. A/d-converter performance evolution. 2007.

[19] Goddard Space Flight Center and United States National Aeronautics and Space Administration. *Significant Accomplishments in Sciences: The Proceedings of a Symposium Held at NASA Goddard Space Flight Center.* NASA SP. Scientific and Technical Information Office, National Aeronautics and Space Administration, 1975.

[20] David M. Pozar. *Microwave Engineering, forth edition.* John Wiley & Sons, Inc., 2011.

[21] Analog Devices. Intermodulation distortion considerations for adcs. October 2008.

[22] Texas Instruments. Lmh6624 and lmh6626 single/dual ultra low noise wideband operational amplifier. November 2002.

[23] Wim C. van Etten. *Introduction to Random Signals and Noise*. Wiley, 2006.

[24] Texas Instruments. Calculating noise figure in op amps.

Appendix A

Appendix

A.1 M-Code: Calculate System Parameters

```
close all;
%This script is meant to calculate the sky noise picked up by the antenna
%The equation is determined empirically and presented in the Daris Report
%Tsky(f)=T1k*{((c)/(f*I0))^2.55+ (f/f0)^1.8} + Tbg
%T1k= 1K
%c= 299792458 m/s
%f0= 10 GHz
%I0= 0.2008 m
%Tbg= 2.7K
%--------------------------------------------------------------------------
%% Import data from text file.
% Script for importing data from the following text file:
%
%    C:\Users\Robert\Dropbox\Master Thesis\Data\COP9M6\Im7cm.csv
%
% To extend the code to different selected data or a different text file,
% generate a function instead of a script.

% Auto-generated by MATLAB on 2016/02/09 11:36:49
close all
%% Initialize variables.
filename = 'C:\Users\Robert\Dropbox\MasterThesis\Data\COP9M6\Im7cm.csv';
delimiter = ',';
startRow = 2;

%% Format string for each line of text:
%   column1: double (%f)
%   column2: double (%f)
% For more information, see the TEXTSCAN documentation.
formatSpec = '%f%f%*s%[^\n\r]';

%% Open the text file.
fileID = fopen(filename,'r');

%% Read columns of data according to format string.
% This call is based on the structure of the file used to generate this
% code. If an error occurs for a different file, try regenerating the code
% from the Import Tool.
dataArray = textscan(fileID, formatSpec, 'Delimiter', delimiter, 'HeaderLines...
    ' ,startRow-1, 'ReturnOnError', false);

%% Close the text file.
fclose(fileID);

%% Post processing for unimportable data.
% No unimportable data rules were applied during the import, so no post
% processing code is included. To generate code which works for
% unimportable data, select unimportable cells in a file and regenerate the
% script.

%% Allocate imported array to column variable names
FreqMHz = dataArray{:, 1};
```

```
52  imZp1 = dataArray{:, 2};
53
54
55  %% Clear temporary variables
56  clearvars filename delimiter startRow formatSpec fileID dataArray ans;
57  %% Initialize variables.
58  filename = 'C:\Users\Robert\Dropbox\MasterThesis\Data\COP9M6\Re7cm.csv';
59  delimiter = ',';
60  startRow = 2;
61
62  %% Format string for each line of text:
63  %   column1: double (%f)
64  %   column2: double (%f)
65  % For more information, see the TEXTSCAN documentation.
66  formatSpec = '%f%f%*s%[^\n\r]';
67
68  %% Open the text file.
69  fileID = fopen(filename,'r');
70
71  %% Read columns of data according to format string.
72  % This call is based on the structure of the file used to generate this
73  % code. If an error occurs for a different file, try regenerating the code
74  % from the Import Tool.
75  dataArray = textscan(fileID, formatSpec, 'Delimiter', delimiter, 'HeaderLines...
        ' ,startRow-1, 'ReturnOnError', false);
76
77  %% Close the text file.
78  fclose(fileID);
79
80  %% Post processing for unimportable data.
81  % No unimportable data rules were applied during the import, so no post
82  % processing code is included. To generate code which works for
83  % unimportable data, select unimportable cells in a file and regenerate the
84  % script.
85
86  %% Allocate imported array to column variable names
87  FreqMHz1 = dataArray{:, 1};
88  reZp1 = dataArray{:, 2};
89
90  load resistances
91  sg= 5.8e7;
92  sigma=repmat(sg,[size(FreqMHz,1) 1]);
93  f=FreqMHz.*1e6;
94  sd=sqrt(2./(2.*pi.*f.*4.*pi.*1e-7.*sigma));
95
96  a=0.1e-3;
97  l=9.6;
98  length=3.0e8./f(end);
99  Rhf=(l/(2*pi*(a/2))).*(sqrt((2.*pi.*f.*4.*pi.*1e-7)./(2*sigma)));
100 RL=0.5*Rhf;
101 Rlf=l./(((a/2).^2.*pi).*sigma);
102 plot(f/1e6,max(Rlf(:,1),Rhf(:,1))/2,'LineWidth',2)
103 ResistanceCopper=max(Rlf(:,1),Rhf(:,1))/2;
104 e=(reZp1-ResistanceCopper)./((reZp1-ResistanceCopper)+ResistanceCopper);
105 e2=reZp1./(reZp1+ResistanceCopper);
106 inputImp=1800
107 Zant=reZp1+i*imZp1
108 Gamma =(Zant-inputImp)./(Zant+inputImp)
109 er=1-abs(Gamma).^2
110 e0=e.*er
111 % plot(f/1e6,e*100)
112 % hold on
113 plot(f/1e6,e*100,'LineWidth',2)
```

```
114 xlabel('Frequency (MHz)')
115 ylabel('Efficiency (%)')
116 axis([1 30 65 100])
117 movegui('north')
118 export_fig('C:\Users\Robert\Dropbox\MasterThesis\Report\Report\Images\chap3\...
        Efficiency', '-pdf', '-transparent')
119
120 T1k= 1;
121 Tphys=293;
122 c= 299792458;
123 f0= 10e9;
124 I0= 0.2008;
125 Tbg= 2.7;
126 %f=0.3e6:0.1e6:30e6;
127
128
129 Tsky=T1k.*(((c)./(f.*I0)).^2.55+ (f./f0).^1.8) + Tbg;
130
131 Tant=e0.*Tsky +(1-e0).*Tphys;
132
133 Rrad=reZp1-ResistanceCopper;
134
135 figure()
136 loglog(f/1e6,Tant,'LineWidth',2)
137 hold on
138 loglog(f/1e6,Tsky,'LineWidth',2)
139 hold on
140 loglog(f/1e6,0.1.*Tant,'LineWidth',2)
141 axis([1e6/1e6 30e6/1e6 1e2 1e9])
142 xlabel('Frequency (MHz)')
143 ylabel('Sky noise temperature (K)')
144 legend({'T_{ant}','T_{Sky}','T_{recMAX}'})
145 ax=gca;
146 ax.XTick=[0.3 0.6 0.9 1.2 1.5 1.8 2.1 2.4 2.7 3 6 9 12 15 18 21 24 27 30];
147 ax.XTickLabel={0.3 '' '' '' '' '' '' '' '' 3 '' '' '' '' '' '' '' '' 30};
148 ax.XGrid= 'on';
149 ax.YGrid= 'on';
150 export_fig('C:\Users\Robert\Dropbox\MasterThesis\Report\Report\Images\chap3\...
        Tant', '-pdf', '-transparent')
151 movegui('southwest')
152
153 G=1.6405.*ones(100,1);
154 lambda=c./f;
155 Aeff=(lambda.^2.*3)./(8.*pi);
156 Pin=Aeff.*10e6.*1e-26.*11000;
157 Pout=8.91e-5;
158 Gain=10.*log10(Pout./Pin);
159 figure();
160 plot(f/1e6,Gain,'LineWidth',2)
161 axis([1 30 60 100])
162 xlabel('Frequency (MHz)')
163 ylabel('Gain (dB)')
164 %export_fig('C:\Users\Robert\Dropbox\Master Thesis\Journal\20160303\Images\...
        Gain', '-pdf', '-transparent')
165 figure();
166 semilogx(f/1e6,Aeff,'LineWidth',2)
167 xlabel('Frequency (MHz)')% G1=Gain-80
168 % G1(G1<0)=0
169 % adj=70-G1
170 % ENOB=(adj-1.76)./6.02
171 % plot(f/1e6,ENOB,'Linewidth',2)
172 % axis([1 30 0 12])
173 % xlabel('Frequency (MHz)')
```

```
% ylabel('Effective number of bits')
% export_fig('C:\Users\Robert\Dropbox\Master Thesis\Journal\20160303\Images\...
    ENOB', '-pdf', '-transparent')
ylabel('A_{eff} (m^2)')
axis([1 30 0 12e3])
ax=gca;
ax.XTick=[0.3 0.6 0.9 1.2 1.5 1.8 2.1 2.4 2.7 3 6 9 12 15 18 21 24 27 30];
ax.XTickLabel={0.3 '' '' '' '' '' '' '' '' 3 '' '' '' '' '' '' '' '' 30};
ax.XGrid= 'on';
ax.YGrid= 'on';
%export_fig('C:\Users\Robert\Dropbox\Master Thesis\Journal\20160303\Images\...
    Aeff', '-pdf', '-transparent')
inputPower=10*log10((((Tant(1)-Tant(end))*(0.5*(30e6-300e3)) + Tant(end)*(30...
    e6-300e3))*1.38e-23)/1e-3);
figure()
plot(f/1e6,er.*100,'LineWidth',2)
hold on
plot(f/1e6,e*100,'LineWidth',2)
axis([1 30 0 100])
xlabel('Efficiency')
ylabel('Frequency')
legend({'e_r','e_{cd}'})
export_fig('C:\Users\Robert\Dropbox\MasterThesis\Report\Report\Images\chap3\...
    EFF', '-pdf', '-transparent')
figure()
NF=10*log10(1+(0.1.*Tant)./290)
plot(f./1e6,NF,'linewidth',2)
axis([1 30 0 20])
xlabel('Frequency (MHz)')
ylabel('Noise Figure (dB)')
export_fig('C:\Users\Robert\Dropbox\MasterThesis\Report\Report\Images\chap3\...
    NF', '-pdf', '-transparent')
Pin=sum(abs(diff(Tant)).*abs(diff(f)))*1.38e-23
PiN=sum(abs(diff(0.1*Tant)).*abs(diff(f)))*1.38e-23
Vin=sqrt(Pin*inputImp)*sqrt(2)
Gain=20*log10(1/Vin)
```

A.2 M-Code: Calculate Amplifier Noise Figure

```
%%

[f,Rs]=ImportRes()
eta=120*pi
C=0.5772
a=0.24e-3;
labda=9.6;
wavelength=3.0e8./(f.*1e6);
l=(0.5*labda)./wavelength;
k=(2*pi)./(0.5*labda);
%b=labda./length;
%l=b.*labda
%k=0.65
l=l*labda
Rrad=(eta/(2*pi)).*(C+ log(k.*l) - cosint(k.*l)+ 0.5*sin(k.*l).*(sinint(2.*k....
    *l)-2.*sinint(k.*l))+0.5.*cos(k.*l).*(C+log(0.5.*k.*l)+cosint(2.*k.*l)-2*...
    cosint(k.*l)));
Rin=(Rrad)./sin(0.5.*k.*l).^2;
plot(abs(Rs-Rin))
%Rs=abs(Rs-Rin)
%%
```

```
20
21 N=size(f,1)
22 k=1.38e-23;
23 T=290;
24 Rt=ones(N,1).*1800;
25 Rf=ones(N,1).*4700;
26 Rg=ones(N,1).*150;
27 %Rs=Rs;
28 in=1.8e-12;
29 un=1e-9;
30
31 c1=un.^2;
32 c2=in.^2.*((Rs.*Rt)./(Rs+Rt)).^2;
33 c3=in.^2.*((Rf.*Rg)./(Rf+Rg)).^2;
34 c4=4*k*T.*Rt.*((Rs)./(Rs+Rt)).^2;
35 c5=4*k*T.*Rg.*((Rf)./(Rf+Rg)).^2;
36 c6=4*k*T.*Rf.*((Rg)./(Rf+Rg)).^2;
37
38 Na=c1+c2+c3+c4+c5+c6;
39 Ni=4*k*T.*Rs.*((Rt)./(Rs+Rt)).^2;
40
41 F=10.*log10(1+(Na./Ni));
42 plot(f,F,'LineWidth',2)
43 axis([1 30 0 20])
44 xlabel('Frequency (MHz)')
45 ylabel('Noise Figure (dB)')
46 export_fig('C:\Users\Robert\Dropbox\MasterThesis\Report\Report\Images\chap3\...
       NFCALC', '-pdf', '-transparent')
47 figure()
48 [a, S]=polyfit(f.*1e6,Rin,20)
49 b=polyval(a,f.*1e6)
50 %plot(f,b)
51 text=[]
52 format long
53 for I=20:-1:0
54     if(a(21-I)>0)
55     text=[text '+']
56     end
57     text=[ text num2str(a(21-I),10) '*pow(freq,' num2str(I) ')']
58 end
59 disp('Niek heeft 20 windingen op 22-04-2016 #yoloswag')
60 f=f.*1e6;
61 test=a(1).*f(50).^20+a(2).*f(50).^19+a(3).*f(50).^18+a(4).*f(50).^17+a(5).*f...
       (50).^16+a(6).*f(50).^15+a(7).*f(50).^14+a(8).*f(50).^13+a(9).*f(50).^12+a...
       (10).*f(50).^11+a(11).*f(50).^10+a(12).*f(50).^9+a(13).*f(50).^8+a(14).*f...
       (50).^7+a(15).*f(50).^6+a(16).*f(50).^5+a(17).*f(50).^4+a(18).*f(50).^3+a...
       (19).*f(50).^2+a(20).*f(50).^1+a(21);
62
63 (1.4902e-137*(15.354e6)^20)-(4.4601e-129*(15.354e6)^19)+(6.1961e-121*15.354e6...
       ^18)-(5.3035e-113*15.354E6^17)+(3.1312e-105*15.354e6^16)-(1.3527E-97*15...
       .354E6^15)+(4.4271E-90*15.354E6^14)-(1.1211E-82*15.354E6^13)+(2.2249E...
       -75*15.354E6^12)-(3.4835E-68*15.354E6^11)+(4.3113E-61*15.354E6^10)-(4...
       .2084E-54*15.354E6^9)+(3.2199E-47*15.354E6^8)-(1.911E-40*15.354E6^7)+(8...
       .6627E-34*15.354E6^6)-(2.9351E-27*15.354E6^5)+(7.21E-21*15.354E6^4)-(1...
       .2289E-14*15.354E6^3)+(1.3576E-08*15.354E6^2)-(0.0086114*15.354E6^1)+(2347...
       .353*15.3541E6^0)
```

A.3 M-Code: Process Simulations

```
close all
%% Import data from text file.
% Script for importing data from the following text file:
%
%    C:\Users\Robert\Dropbox\Master Thesis\Data\PEC5M\s11\3cm.csv
%
% To extend the code to different selected data or a different text file,
% generate a function instead of a script.

% Auto-generated by MATLAB on 2016/01/05 10:08:14
fn={'3cm';'7cm';'10cm';'15cm';'25cm';'35cm'}
s11=[];
impre=[];
impim=[];
%% Initialize variables.
for I=1:size(fn,1)
filename = ['C:\Users\Robert\Dropbox\MasterThesis\Data\PEC9M6N\s11\' char(fn(...
    I)) '.csv'];
delimiter = ',';
startRow = 2;

%% Format string for each line of text:
%   column1: double (%f)
%   column2: double (%f)
% For more information, see the TEXTSCAN documentation.
formatSpec = '%f%f%*s%[^\n\r]';

%% Open the text file.
fileID = fopen(filename,'r');

%% Read columns of data according to format string.
% This call is based on the structure of the file used to generate this
% code. If an error occurs for a different file, try regenerating the code
% from the Import Tool.
dataArray = textscan(fileID, formatSpec, 'Delimiter', delimiter, 'HeaderLines...
    ' ,startRow-1, 'ReturnOnError', false);

%% Close the text file.
fclose(fileID);

%% Post processing for unimportable data.
% No unimportable data rules were applied during the import, so no post
% processing code is included. To generate code which works for
% unimportable data, select unimportable cells in a file and regenerate the
% script.

%% Allocate imported array to column variable names
FreqMHz = dataArray{:, 1};
dBS1 = dataArray{:, 2};
s11=[s11 dBS1];

%% Clear temporary variables
clearvars filename delimiter startRow formatSpec fileID dataArray ans;
filename = ['C:\Users\Robert\Dropbox\MasterThesis\Data\PEC9M6N\ImpRe\' char(...
    fn(I)) '.csv'];;
delimiter = ',';
startRow = 2;

%% Format string for each line of text:
%   column1: double (%f)
%   column2: double (%f)
% For more information, see the TEXTSCAN documentation.
formatSpec = '%f%f%*s%[^\n\r]';
```

```
61
62 %% Open the text file.
63 fileID = fopen(filename,'r');
64
65 %% Read columns of data according to format string.
66 % This call is based on the structure of the file used to generate this
67 % code. If an error occurs for a different file, try regenerating the code
68 % from the Import Tool.
69 dataArray = textscan(fileID, formatSpec, 'Delimiter', delimiter, 'HeaderLines...
       ' ,startRow-1, 'ReturnOnError', false);
70
71 %% Close the text file.
72 fclose(fileID);
73
74 %% Post processing for unimportable data.
75 % No unimportable data rules were applied during the import, so no post
76 % processing code is included. To generate code which works for
77 % unimportable data, select unimportable cells in a file and regenerate the
78 % script.
79
80 %% Allocate imported array to column variable names
81 FreqMHz1 = dataArray{:, 1};
82 reZport1_T1 = dataArray{:, 2};
83 impre=[impre reZport1_T1];
84 clearvars filename delimiter startRow formatSpec fileID dataArray ans;
85 %% Initialize variables.
86 filename = ['C:\Users\Robert\Dropbox\MasterThesis\Data\PEC9M6N\ImpIm\' char(...
       fn(I)) '.csv'];
87 delimiter = ',';
88 startRow = 2;
89
90 %% Format string for each line of text:
91 %   column1: double (%f)
92 %   column2: double (%f)
93 % For more information, see the TEXTSCAN documentation.
94 formatSpec = '%f%f%*s%[^\n\r]';
95
96 %% Open the text file.
97 fileID = fopen(filename,'r');
98
99 %% Read columns of data according to format string.
100 % This call is based on the structure of the file used to generate this
101 % code. If an error occurs for a different file, try regenerating the code
102 % from the Import Tool.
103 dataArray = textscan(fileID, formatSpec, 'Delimiter', delimiter, 'HeaderLines...
       ' ,startRow-1, 'ReturnOnError', false);
104
105 %% Close the text file.
106 fclose(fileID);
107
108 %% Post processing for unimportable data.
109 % No unimportable data rules were applied during the import, so no post
110 % processing code is included. To generate code which works for
111 % unimportable data, select unimportable cells in a file and regenerate the
112 % script.
113
114 %% Allocate imported array to column variable names
115 FreqMHz2 = dataArray{:, 1};
116 imZport1_T1 = dataArray{:, 2};
117 impim=[impim imZport1_T1];
118 clearvars filename delimiter startRow formatSpec fileID dataArray ans;
119 end
120 for I=1:size(s11,2)
```

```
121     plot(FreqMHz,s11(:,I),'LineWidth',2)
122     hold on;
123 end
124 %axis([1 30 -20e-6 5e-6])
125 xlabel('Frequency (MHz)')
126 ylabel('s11 (dB)')
127 legend(fn,'location','southeast')
128 export_fig('C:\Users\Robert\Dropbox\MasterThesis\Report\Report\Images\chap4\9...
        m6s11', '-pdf', '-transparent')
129 figure()
130 for I=1:size(s11,2)
131     plot(FreqMHz,impre(:,I),'LineWidth',2)
132     hold on;
133 end
134 %axis([1 30 -30 5])
135 xlabel('Frequency (MHz)')
136 ylabel('Resistance (ohm)')
137 legend(fn,'location','southeast')
138 export_fig('C:\Users\Robert\Dropbox\MasterThesis\Report\Report\Images\chap4\9...
        m6ImpRe', '-pdf', '-transparent')
139 figure()
140 for I=1:size(s11,2)
141     plot(FreqMHz,impim(:,I),'LineWidth',2)
142     hold on;
143 end
144 %axis([1 30 -12e5 0])
145 xlabel('Frequency (MHz)')
146 ylabel('Reactance (ohm)')
147 legend(fn,'location','southeast')
148 export_fig('C:\Users\Robert\Dropbox\MasterThesis\Report\Report\Images\chap4\9...
        m6ImpIm', '-pdf', '-transparent')
```

A.4 M-Code: Process Amplifier Simulations

```
1  close all;
2  clear all;
3  %% Import data from text file.
4  % Script for importing data from the following text file:
5  %
6  %    C:\Users\Robert\Dropbox\MasterThesis\Data\NFSim\NF.csv
7  %
8  % To extend the code to different selected data or a different text file,
9  % generate a function instead of a script.
10
11 % Auto-generated by MATLAB on 2016/05/31 10:19:56
12
13 %% Initialize variables.
14 filename = 'C:\Users\Robert\Dropbox\MasterThesis\Data\NFSim\NF.csv';
15 delimiter = {',',' '};
16 startRow = 12;
17
18 %% Format string for each line of text:
19 %   column1: double (%f)
20 %   column3: double (%f)
21 % For more information, see the TEXTSCAN documentation.
22 formatSpec = '%f%*s%f%*s%[^\n\r]';
23
24 %% Open the text file.
25 fileID = fopen(filename,'r');
26
```

```
27 %% Read columns of data according to format string.
28 % This call is based on the structure of the file used to generate this
29 % code. If an error occurs for a different file, try regenerating the code
30 % from the Import Tool.
31 dataArray = textscan(fileID, formatSpec, 'Delimiter', delimiter, 'HeaderLines...
       ' ,startRow-1, 'ReturnOnError', false);
32
33 %% Close the text file.
34 fclose(fileID);
35
36 %% Post processing for unimportable data.
37 % No unimportable data rules were applied during the import, so no post
38 % processing code is included. To generate code which works for
39 % unimportable data, select unimportable cells in a file and regenerate the
40 % script.
41
42 %% Allocate imported array to column variable names
43 f1 = dataArray{:, 1};
44 NF = dataArray{:, 2};
45
46
47 %% Clear temporary variables
48 clearvars filename delimiter startRow formatSpec fileID dataArray ans;
49 %% Import data from text file.
50 % Script for importing data from the following text file:
51 %
52 %    C:\Users\Robert\Dropbox\MasterThesis\Data\NFSim\Gain.csv
53 %
54 % To extend the code to different selected data or a different text file,
55 % generate a function instead of a script.
56
57 % Auto-generated by MATLAB on 2016/05/31 10:24:58
58
59 %% Initialize variables.
60 filename = 'C:\Users\Robert\Dropbox\MasterThesis\Data\NFSim\Gain.csv';
61 delimiter = {',',' '};
62 startRow = 12;
63
64 %% Format string for each line of text:
65 %   column1: double (%f)
66 %   column3: double (%f)
67 % For more information, see the TEXTSCAN documentation.
68 formatSpec = '%f%*s%f%*s%[^\n\r]';
69
70 %% Open the text file.
71 fileID = fopen(filename,'r');
72
73 %% Read columns of data according to format string.
74 % This call is based on the structure of the file used to generate this
75 % code. If an error occurs for a different file, try regenerating the code
76 % from the Import Tool.
77 dataArray = textscan(fileID, formatSpec, 'Delimiter', delimiter, 'HeaderLines...
       ' ,startRow-1, 'ReturnOnError', false);
78
79 %% Close the text file.
80 fclose(fileID);
81
82 %% Post processing for unimportable data.
83 % No unimportable data rules were applied during the import, so no post
84 % processing code is included. To generate code which works for
85 % unimportable data, select unimportable cells in a file and regenerate the
86 % script.
87
```

```
%% Allocate imported array to column variable names
f2 = dataArray{:, 1};
Gain = dataArray{:, 2};


%% Clear temporary variables
clearvars filename delimiter startRow formatSpec fileID dataArray ans;
plot(f1,NF,'LineWidth',2)
axis([1 30 0 30])
xlabel('Frequency (MHz)')
ylabel('Noise Figure (dB)')
export_fig('C:\Users\Robert\Dropbox\MasterThesis\Report\Report\Images\chap4\...
    NF', '-pdf', '-transparent')
figure()
plot(f2,Gain,'LineWidth',2)
axis([1 30 0 100])
xlabel('Frequency (MHz)')
ylabel('Voltage Gain (dB)')
export_fig('C:\Users\Robert\Dropbox\MasterThesis\Report\Report\Images\chap4\...
    Gain', '-pdf', '-transparent')
```

```
%% Import data from text file.
% Script for importing data from the following text file:
%
%    C:\Users\Robert\Dropbox\MasterThesis\Data\NFSim\Gain.csv
%
% To extend the code to different selected data or a different text file,
% generate a function instead of a script.

% Auto-generated by MATLAB on 2016/05/31 10:24:58

%% Initialize variables.
filename = 'C:\Users\Robert\Dropbox\MasterThesis\Data\NFSim\Gain.csv';
delimiter = {',',' '};
startRow = 12;

%% Format string for each line of text:
%   column1: double (%f)
%   column3: double (%f)
% For more information, see the TEXTSCAN documentation.
formatSpec = '%f%*s%f%*s%[^\n\r]';

%% Open the text file.
fileID = fopen(filename,'r');

%% Read columns of data according to format string.
% This call is based on the structure of the file used to generate this
% code. If an error occurs for a different file, try regenerating the code
% from the Import Tool.
dataArray = textscan(fileID, formatSpec, 'Delimiter', delimiter, 'HeaderLines...
    ' ,startRow-1, 'ReturnOnError', false);

%% Close the text file.
fclose(fileID);

%% Post processing for unimportable data.
% No unimportable data rules were applied during the import, so no post
% processing code is included. To generate code which works for
% unimportable data, select unimportable cells in a file and regenerate the
% script.

%% Allocate imported array to column variable names
```

```
41 f = dataArray{:, 1};
42 Gain = dataArray{:, 2};
43
44
45 %% Clear temporary variables
46 clearvars filename delimiter startRow formatSpec fileID dataArray ans;
```